Evaluation of Emerging Technologies on a 1.6 L Turbocharged GDI Engine

Graham Conway[a,*], Dennis Robertson[a], and Chris Chadwell[a], Joseph McDonald[b], John Kargul[b], Daniel Barba[b], and Mark Stuhldreher[b]

[a] Southwest Research Institute

[b] US Environmental Protection Agency

[*] **Contact Information** For additional information, please contact **Graham Conway,** Southwest Research Institute, graham.conway@swri.org

Abstract

Low-pressure loop exhaust gas recirculation (LP- EGR) combined with higher compression ratio, is a technology package that has been a focus of research to increase engine thermal efficiency of downsized, turbocharged gasoline direct injection (GDI) engines. Research shows that the addition of LP-EGR reduces the propensity to knock that is experienced at higher compression ratios [1]. To investigate the interaction and compatibility between increased compression ratio and LP-EGR, a 1.6 L Turbocharged GDI engine was modified to run with LP-EGR at a higher compression ratio (12:1 versus 10.5:1) via a piston change. This paper presents the results of the baseline testing on an engine run with a prototype controller and initially tuned to mimic an original equipment manufacturer (OEM) baseline control strategy running on premium fuel (92.8 anti-knock index). This paper then presents test results after first adding LP-EGR to the baseline engine, and then also increasing the compression ratio (CR) using 12:1 pistons. As a last step, the 10.5 CR engine with LP-EGR was run on regular fuel (87.7 anti-knock index) to verify that this configuration could be calibrated to maintain performance like the baseline engine running on premium fuel. To understand the effect of each technology and operating strategy combination on vehicle fuel economy, the various engine maps were compared in EPA's Advanced Light-Duty Powertrain and Hybrid Analysis (ALPHA) tool over U.S. regulatory drive cycles. This work was done in close collaboration with U.S. EPA engineers as part of their continuing assessment of advanced light-duty automotive technologies to support setting appropriate national greenhouse gas standards.

Introduction

By 2025, the automotive industry will be required to have reduced carbon dioxide (CO2) emissions by at least 30% and non-methane organic gases and oxides of nitrogen (NMOG+NO_x) by 80% [2, 3]. A commonly used strategy to improve fleet-wide emissions reduction is engine downsizing. A downsized engine has a reduced engine displacement but a higher specific power, usually via forced induction to maintain overall performance. By reducing engine displacement, the engine can operate at a higher, more efficient load to produce the same vehicle-required power, thus giving an overall efficiency improvement. However, operating the engine at higher loads will increase the propensity for engine knock to occur. Knock can be mitigated by retarding ignition timing to permit higher load operation but with reduced efficiency. One other method to increase efficiency is to increase the geometric compression ratio (CR). However, high compression ratios also raise compression temperatures, which can increase knock propensity. Thus, the CR on highly boosted, downsized engines is limited to avoid engine knock.

One promising strategy to increase efficiency on downsized engines is the use of cooled exhaust gas recirculation (EGR). Cooled EGR leads to higher thermal efficiencies through a reduction in heat transfer losses as well as improving the working fluid. One further benefit of cooled EGR is a reduction in knock, which enables higher CRs and more optimized combustion phasing [4, 5, 6, 7, 8, 9, 10, 11]. EGR can reduce knock propensity through thermodynamic cooling and chemical effects. The high specific heat capacity of CO_2 and H_2O reduces the temperature driving autoignition reactions. Regarding chemical effects, there are several aspects. Firstly, the reduction of O_2 with dilution does not significantly contribute to reduced knock propensity in single-stage autoignition fuels, such as gasoline [8]. Trace species of unburned HC, CO or NO can advance or retard the onset of knock depending on the fuel type. There is ongoing debate regarding the significance of EGR and knock mitigation depending on the test fuel and pressure, temperature operating region. Research has attribute the effectiveness of EGR to the fuel and pressure, temperature history of the gas [5, 7, 9]. At high pressure conditions, the effectiveness of EGR to mitigate autoignition reduces [7] and therefore the relevance of cooled LP-EGR on boosted engines may be less significant.

Cooled EGR also offers specific- heat related benefits by displacing the diatomic air molecules with triatomic molecules circulated back from the exhaust. The increase in heat capacity results in reduced combustion temperatures leading to lower NOX, CO and PM emissions [12, 13, 14]. As a diluent, the use of cooled EGR can provide a pumping benefit, although at lower loads, where pumping is a primary concern, internal trapped residuals are favored over external EGR [15]. Overall, the level of improvement from adding EGR to a gasoline engine, independent of other considerations such as downsizing or hybridization or separate pumping loss mitigation technologies (i.e. variable valve lift and duration, late/early intake valve closing, etc.), has been shown to be approximately 6-8% on cycles such as the New European Driving Cycle (NEDC) [14] and potentially more on more highly loaded cycles such as the Federal Test Procedure (FTP-75). Certainly, cooled EGR concepts are becoming more prevalent as evidenced by several production applications for high efficiency spark ignited (SI) engines [16, 17].

Another potential efficiency path is by reducing the effective CR of the engine but maintaining a high expansion ratio. Some recent production engines and research [18, 19, 20] employ a Miller or Atkinson-cycle strategy where the intake valve is closed before or after piston bottom-dead-center (BDC) to reduce the effective CR, which avoids knock but maintains the high expansion ratio to realize efficiency. A challenge of Miller or Atkinson-cycle operation is a reduction in charge motion, required for fuel mixing and fast burn rates, as well as low volumetric efficiency which leads to higher boost requirements.

Like Miller-cycle operation, the use of cooled EGR reduces the mass of fresh air available for combustion, thus limiting engine performance. To increase the density of the charge, turbocharging and intercooling are commonly used to increase the pressure and reduce the temperature, respectively. A boost device such as a turbocharger converts exhaust enthalpy into useful work compressing air on the intake side. EGR leads to cooler exhaust temperatures and therefore lower exhaust enthalpy. The combination of high pressure ratio and low exhaust enthalpy generally requires a smaller compressor and turbine wheel to achieve the low engine speed brake mean effective pressure (BMEP) targets. At higher speeds, the device may be undersized, and the compressor would choke under the flow demands. It is difficult to use a single-boosting device to meet both low and high-speed performance targets. One solution is to use two or more turbochargers of varied sizes. A smaller turbocharger provides boost at lower engine speeds, while a larger turbocharger has the flow capacity at higher

engine speeds. The use of two boost devices may not be ideal owing to cost and packaging implications. Variable nozzle turbines (VNTs) are turbochargers that adjust their effective turbine size by adjusting internal flow paths; VNTs are appearing on light-duty gasoline engines [18]. VNT technology may permit the engine to operate with EGR and maintain peak performance with a single boosting device [21]. EPA does expect 48 V mild hybrid technology to become increasingly common as a greenhouse gas (GHG)-reducing technology [22]. If 48 V is already available on a vehicle, there may still be low speed performance advantages to using an e-booster, particularly in truck or high-performance applications.

Regarding fuel quality and autoignition, the predominant use of regular-grade, 87-88 anti-knock-index (AKI) gasoline in the U.S. must be considered for future studies into engine hardware. Autoignition occurs when low-temperature exothermic reactions occur in the unburned mixture end-gas. If the heat release is severe enough, and enough fuel is burned, then engine knock can occur. It is possible to reduce the likelihood of autoignition occurring by altering fuel chemistry. Premium-grade gasoline, typically 92 - 93 AKI in the U.S., has a higher resistance to autoignition and knock compared to regular-grade gasoline. Ignition retard is typically required to avoid engine knock at higher BMEP. Ignition retard offsets the combustion event to reduce heat addition. Retarding ignition timing reduces overall efficiency however by lowering the effective expansion ratio and reducing combustion efficiency. Therefore, to maintain a target load, more air must be inducted to permit additional fuel and maintain stoichiometric combustion. If a regular grade fuel is used, then additional combustion retard may be required, placing an additional requirement on the boosting system. When considering whether EGR is compatible with high CR, it is necessary to evaluate both regular and premium fuels to understand the boosting requirements.

Experimental Setup

The engine used in these experiments is based on a PSA[1] EP6CDTX engine. It is a 4 cylinder, 1.6 L engine (Figure 1, Table 1) equipped with intake and exhaust cam phasing, continuously variable valve lift (CVVL) on the intake and a twin-scroll turbocharger with non-integrated, steel-cast exhaust manifold. The engine is equipped with a side-mounted injector located under the intake ports and normally operates with early injection timing fuel-air equivalence ratio (φ) of approximately 1.0. The relevant hardware characteristics of the engine are shown in Table 1.

The operating ranges of the CVVL system and the dual cam-phasers are described in Figure 2. The parked position of the exhaust cam phaser yielded earliest exhaust phasing with the maximum valve lift location at 114° before top dead center (bTDC). The parked intake cam phaser position was set to provide latest intake cam phasing with the maximum valve lift location at 115° after top dead center (aTDC) (if commanded valve lift setting is at maximum lift of 9.1 mm since the valve phasing angles such as valve opening and closing angles are also dependent on the nominal valve lift settings). The CVVL system offered the ability to vary the nominal valve lift continuously between 0.2 mm and 9.1 mm.

The engine was modified with a LP-EGR system. Due to the challenges in boosting high dilution engines [21], a two-stage boosting system was added, consisting of a positive displacement Eaton supercharger unit for the low stage. The series production twin-scroll turbocharger with electronic wastegate was used for the high stage. The supercharger was set up so that it could be bypassed completely when not required. For this experiment, the three-way catalyst (TWC) was not present, and EGR was therefore

[1] Peugeot Société Anonyme - manufacturer of Peugeot and Citroen vehicles

considered pre-TWC EGR. System back pressure simulated the presence of a TWC by way of a restricting valve placed at the end of the exhaust system.

The EGR cooler was run as part of the engine coolant circuit and the EGR coolant flow was set to maintain an EGR gas outlet temperature of less than 200 °C at rated power. For all the testing discussed in this report, an air-to-liquid charge air cooler was employed and the intake manifold temperature was maintained at 40 °C. Coolant and oil temperatures were set in two stages. Below 3000 rpm and engine load below 11 bar BMEP, oil and coolant temperatures were set to 100 °C. At all other conditions oil and coolant temperature were set to 85 °C. Temperatures were controlled via Proportional-Integral-Derivative (PID)-actuated flow valves to vary the flow rate of ambient temperature water to the liquid-to-liquid heat exchangers for the oil, coolant and manifold. The engine installation in the test cell can be seen in Figure 3.

To study the effect of CR changes, two pistons were used in this study. The first piston was the stock piston with a CR of 10.5:1. The second piston was designed to provide a CR 12.0:1, achieved by reducing the piston bowl in comparison to the stock piston, as shown in Figure 4.

A comprehensive set of instrumentation was included for this experiment, with low-speed pressure and temperature measurement equipment placed around the engine (e.g., ambient test cell conditions, intake and exhaust system, cooling system, etc.) to identify absolute values as well as pressure and temperature changes. For high speed measurement, an encoder was used with 0.5°/ crank angle (CA) resolution while in-cylinder pressure was measured via four Kistler 6041B piezo-electric transducers calibrated to 120 bar.

Test Methodology

For this study, three brake-specific fuel consumption (BSFC) maps were generated for the three different engine configurations:

1. No EGR and CR 10.5:1 (stock configuration and baseline)
2. LP-EGR and CR 10.5:1
3. LP-EGR and CR 12.0:1

A total of 65 points were logged for each configuration, test points were weighted to give high-resolution in drive-cycle regions while also providing data at full-load conditions as shown in Figure 5. At each test point, data were averaged over 60 seconds to log low-speed data and 300 cycles were acquired for high-speed data. Only one data point was logged per speedload point, per configuration. To ensure the engine baseline behavior remained constant throughout the test a daily check point was run. The coefficient of variability of brake specific fuel consumption was less than 1.3% for 50 test points.

For the baseline engine configuration, actuator positions were set based on data supplied by the engine manufacturer. The actuator positions were assumed to provide best BSFC at steady-state operating conditions. For engine configuration 2, the addition of LP-EGR required re-targeting of actuator positions to achieve best BSFC under all conditions. Engine speed was controlled via an eddy-current dynamometer. Primary engine load was controlled based on the following strategies:

1. Intake valve height varied to achieve target BMEP. Main throttle controlled manifold air pressure (MAP) to 93 kPa.
2. Once the intake valve reached the maximum 9.1 mm, the main throttle opened to achieve target load
3. At above atmospheric pressure, the turbocharger wastegate was closed until the target load was reached.
4. If load could not be achieved with the turbocharger, the supercharger by-pass valve closed and the supercharger speed increased to further increase airflow

Start of injection (SOI) timing observed in the baseline engine at various speeds and loads was also used for the two LP-EGR engine configuration tests. The remaining actuators (intake cam advance, exhaust cam retard, and external LP-EGR amount) were adjusted to target lowest BSFC for the two LP-EGR engine configuration cases. The approach used a Box-Behnken design of experiments (DoE) to produce response surfaces of valve lift, valve overlap and BSFC at various EGR and exhaust cam retards as shown in Figure 6.

The data sampling process involved taking 27 test points manually targeting the upper and lower ranges of the four different variables under 15 speed-load conditions. Once mapped, the data were used to provide optimum controller set points at each of the 15 speed-load points to achieve lowest BSFC. Secondary checks were then performed on the engine to ensure that the BSFC response matched the model prediction. The optimum settings were interpolated across the test point range to give target actuator settings at each speedload case.

Combustion phasing was adjusted to knock limited spark advance (KLSA) and/or to yield an optimal location of CA50 (50% burn relative to crank-angle), which is 6-8° aTDC for this engine. Fuel flow was measured using a Micro Motion CMF10M Coriolis flow meter (Emerson/Micro Motion, St. Louis, MO). Exhaust samples were taken with a heated sample line and five gaseous emissions (CO, HC, NOx, CO2, O2) were quantified using a Horiba MEXA-7100 suite of gas analyzers (Horiba, Ltd., Kyoto, Japan). CO_2 was directly measured in the intake manifold and analyzed by the same Horiba analyzer to provide the EGR rate. Note that the EGR rate is calculated by dividing the CO2 level in the intake manifold by the exhaust CO2 level (after correcting for ambient CO_2 levels), so the EGR rate was a volumetric rate and not a mass rate (see Equation 1).

$$EGR_{rate} = \frac{(EGR_{int} - EGR_{atm})}{(EGR_{exh} - EGR_{atm})} \cdot 100 \qquad (1)$$

The fuel chosen for the BSFC mapping was the EPA Tier II fuel. For the second phase of testing, LEV III regular fuel with 10% ethanol, by volume, was used. Specifications for each fuel can be seen in Table 2.

Drive Cycle Modeling

GHG emissions over the U.S. regulatory drive cycles were modeled using the EPA Advanced Light-Duty Powertrain and Hybrid Analysis (ALPHA) tool [23, 24, 25]. ALPHA is a physics based, forward-looking, full vehicle computer simulation capable of analyzing various vehicle types combined with different powertrain technologies. The software tool is a MATLAB/Simulink based desktop application. The ALPHA model includes simulation of realistic vehicle behavior and internal auditing of all vehicle energy flows [25]. For consistency with current EPA GHG emissions compliance requirements, drive cycle modeling assumed use of Tier 2 certification fuel.

Results and Discussion

The following sections are provided to compare no-EGR with LP-EGR as well as the performance of a low and high CR with LP-EGR.

CR 10.5:1 with and without LP-EGR

The baseline BSFC map can be seen in Figure 7. The best BSFC of 233 g/kWh (35.8% brake thermal efficiency or BTE) was achieved at 2500 rpm 12 bar BMEP. At 2000 rpm 2 bar BMEP, the engine achieved 337.0 g/kWh (24.7% BTE). Optimal combustion phasing could be achieved up until 12 bar BMEP at engine speeds greater than 1500 rpm; this operating load is defined as maximum brake torque (MBT) timing. This condition indicates the load at which an engine can operate, with optimal combustion, without knocking. After MBT, spark timing was retarded to avoid engine knock.

The BSFC map generated with the addition of cooled external LP-EGR can be seen in Figure 8. A minimum BSFC of 222.5 g/kWh (37.5% BTE) was achieved at 2750 rpm 14 bar BMEP, representing a 4.5% increase in BTE compared to the no EGR case. The increase in BTE can be attributed to the two main benefits of LP-EGR: reduced heat transfer and reduced knock propensity. The benefit of reduced knock propensity from LP-EGR can be deduced by the increase in load (14 bar BMEP) at which the lowest BSFC was achieved compared to the no-EGR configuration.

The maximum load at MBT line with LP-EGR was 15 bar BMEP, after 1500 rpm an increase of 4 bar BMEP over the non-EGR condition. At 2000 rpm and 2 bar BMEP, the best BSFC was 333.2 g/kWh (25% BTE). The difference between the two configurations at this low-load point was 1.1%, lower than the benefit observed at higher loads.

The use of a CVVL system on the engine removes the opportunity to take full advantage of one of the benefits of LP-EGR: pumping loss reduction. A small pumping benefit is still observed because the dilution effect of LP-EGR requires that a higher intake valve lift be used for the LP-EGR case compared to the non-EGR case. However, because the change in pumping work occurs at the intake valve rather than the main throttle, the benefit is smaller. A secondary reason for the lack of BSFC improvement at lower loads for the LP-EGR configuration can be seen in Figure 9 where only a small amount of external EGR is used at the 2000 rpm 2 bar case. External cooled EGR is not used at low loads as it is more efficient to trap hot internal EGR by employing large amounts of valve overlap. The hot internal EGR increases overall cylinder temperatures which increases dilution tolerance and combustion speed by having uncatalyzed H_2, HC and CO present. The presence of these species speed up oxidation reactions and can increase laminar burning velocity enabling a greater total dilution (internal + external) than when using cooler EGR alone. Additionally, trapped EGR does not have to travel through the EGR cooler or valve and therefore has lower overall engine pumping and heat losses than external EGR. The cumulative benefits of internal EGR can improve efficiency by approximately 0.5% -1% compared to external cooled EGR [26].

External cooled LP-EGR is beneficial at higher engine loads where the knock reduction permits optimal combustion phasing as well as lowering heat transfer. The improved BSFC is likely caused by the greater valve overlap for the EGR case, which results in greater total trapped dilution. The ability to run with higher total dilution was enabled by the marginally higher energy ignition system used for engine Configuration 2 compared to the baseline engine configuration.

The difference in CA50 for the two configurations is shown in Figure 10. At the low-speed/low-load condition, the combustion phasing remained the same for the two engine configurations, as neither was knock limited. At high-speed/low-load, there appears to be a later combustion phasing for the EGR condition. The cause was not considered to be combustion related as the engine was not knock limited at this condition. The likely cause was a controller set point error, not considered a significant observation as it is unlikely that engine knock required combustion retard for the EGR configuration test. Indeed, the difference in CA50 would cause a small difference in BSFC where CA50 is near optimum timing. However, the impact over regulatory drive cycles is also thought to be low due to the low residence time at high-speed, low-load conditions.

As engine load increases, combustion phasing can be up to eight degrees more advanced for the LP-EGR case (20° aTDC) compared to the non-EGR configuration (28° aTDC), which yields a significant BSFC benefit. Figure 10 also shows that at the low-speed high-load region, CA50 is advanced for the non-EGR case. As this region is the most influenced by engine-knock, it might be surprising to see comparable CA50 timings in this region. The early CA50 timings can be explained by the baseline calibration strategy.

The OEM strategy for the engine was to run in a tail-pipe lean mode in this region, commonly seen on European engine calibrations. The lean tailpipe condition is caused by lean-scavenging where a positive delta pressure across the head, coupled with valve overlap, results in fresh air passing through the exhaust valve during the gas exchange process. By removing hot residuals, the propensity to knock is reduced and combustion phasing can be advanced. The downside of this strategy is that the high O_2 levels in the exhaust prevent TWC reduction reactions taking place, and any NO_x present in the exhaust will slip through the TWC. This strategy will no longer be compliant with the introduction of Real Driving Emission (RDE) regulations in Europe which will monitor emissions over a wider operating window of the map. This strategy is also not typical for U.S. operation, as it is regulated under U.S. auxiliary emission control device (AECD) and defeat device provisions. U.S. and California emissions standards require operation at slightly net-rich of $\varphi = 1$ for use of TWC as the primary NOx emissions control. This strategy enables full-load performance to be maintained but with an efficiency penalty. The baseline engine equivalence ratio can be seen in Figure 11.

A BSFC comparison map between Configuration 1 (baseline) and Configuration 2 (10.5 CR with LP-EGR) can be seen in Figure 12. Generally, the addition of LP-EGR resulted in a BSFC benefit under almost all conditions across the map; on average, the addition of LP-EGR gave a 4.5% BSFC reduction. The benefits of EGR are most significant at high loads where knock can be mitigated and a more advanced CA50 can be targeted. At lower loads, the benefits are small on this engine as internal residuals are utilized rather than external LP-EGR.

As a diluent, LP-EGR replaces fresh air with charge composition that does not take part in the combustion process. To maintain a constant load while adding EGR, it is necessary to increase the density of the fresh charge to enable the same fresh air mass as if EGR were not present. For a given mass flow requirement, there is therefore a higher-pressure ratio requirement from the compressor making boosting a challenge.

The addition of LP-EGR also reduces exhaust gas temperatures (EGTs) and therefore the exhaust enthalpy required to drive the turbine. To overcome these challenges, the supercharger was used. For this study, the supercharger was driven via an electric motor powered by a separate test cell electrical supply. When running the experiment, exhaust back pressure was matched to intake pressure to more

closely resemble a matched turbocharger system. The gauge pressure supplied by the supercharger is shown in Figure 13. The 1750 rpm/20 bar BMEP operating point required a significant amount of power (over 10 kW) from the external supplied boost device. Power consumption was not measured but can be approximately calculated based on the isentropic compression law through measured head addition through the compression stage and assuming a supercharger efficiency.

Although it is likely that the engine efficiency would be significantly lower when accounting for the power required to run the supercharger, no attempt was made in this paper to quantify that impact. Instead, this issue is addressed in a related paper that explores the use of variable turbine geometry turbocharger operating across the entire engine map [21].

CR 12.0:1 and CR 10.5:1 with LP-EGR

For Configuration 3, the engine CR was increased to 12:1 and the mapping process was repeated. Actuators were set to identical values compared to Configuration 2 with the exception of spark-timing, which was again targeted to KLSA or optimum combustion phasing.

The final BSFC map for Configuration 3 can be seen in Figure 14. The lowest BSFC of 220.0 g/kWh (37.8% BTE) occurred at 2500 rpm 12 bar BMEP, a 1.2% reduction over the lowest BSFC observed for the CR 10.5:1 case with LP-EGR or 5.4% over the baseline case without EGR. The 2000 rpm and 2 bar BMEP case also improved with the increase in CR with the lowest BSFC of 320.1 g/kWh (26.0% BTE) representing a 3.9% and 5.0% improvement over Configuration 2 and 1, respectively.

The expansion ratio increased with the CR increase, thereby extracting additional heat (work) from the combustion process resulting in the improved efficiency. From the Otto-Cycle efficiency formula [27], the expected benefit would only be approximately 2% to the lower CR case. The EGT for the 12.0:1 configuration was 26 °C lower than for the 10.5:1 case, further supporting a quantifiable higher efficiency for the 12.0:1 configuration.

Additionally, the crank angle degree duration between 10% and 90% of the fuel being burned (MFB 10-90) was three crank angle degrees shorter for the high CR case that would contribute to an efficiency benefit.

The maximum load MBT timing line for the high CR configuration was reduced to 10 bar BMEP above 1500 rpm, a level similar to the level seen in Configuration 1 (baseline). The reduction in the maximum load at the MBT timing line is not surprising, as the higher CR leads to higher in-cylinder temperatures, resulting in engine knock.

The BSFC comparison map between the two LP-EGR configurations can be seen in Figure 15. Clearly, BSFC values at conditions below 10-12 bar BMEP are lower for the CR 12.0:1 configuration. Knock is more obvious above 12 bar BMEP and despite the same EGR levels (see Figure 16). CA50 must be retarded, as can be seen in Figure 17.

The most significant observation is that BSFC is significantly higher under conditions approaching full load (16 bar BMEP and above). The reason for the increased BSFC values can be seen in the EGR map. The LP-EGR rate was significantly lower above 16 bar BMEP compared to the lower CR configuration. Reducing the LP-EGR rate led to an increase in heat transfer and therefore lower efficiency. More significantly, the reduction of LP-EGR resulted in increased knock activity. Combustion phasing retard

was required to avoid knock. The lower EGR and later combustion phasing result in high BSFC values at high loads for the 12.0:1 CR configuration.

Traditionally, LP-EGR is used to abate knock and permit an increase in CR. This was not the case for the current study at 12.0:1 CR. As engine load increased, knock was encountered and CA50 was retarded to mitigate knock but the engine reached the combustion stability threshold of 3% coefficient of variance (CoV) of indicated mean effective pressure (IMEP). Therefore further combustion retard was not possible once a CoV of 3% was reached. To increase load it was necessary to remove EGR to permit further timing retard. Ultimately, at the high load conditions, almost all external EGR had to be removed from the engine to permit enough retard to avoid knock at the target load. This result suggests that there is a load limit defined by CR and dilution tolerance. A graphical representation of this phenomenon can be seen in Figure 18. The four points shown in the figure are detailed below.

1. 20 bar BMEP is achieved for a non-EGR engine at a CR 10.5:1 CR. Due to knock, combustion phasing is retarded with a CA50 of 23° aTDC. The CoV limited combustion at the same load is approximately a CA50 of 35° aTDC, i.e., there are 10 crank angle degrees (CAD) available to retard combustion phasing before the engine reaches a stability limit.
2. Assume 20% LP-EGR has been added to the engine. The 20 bar BMEP can still be achieved, with the reduced knock propensity the CA50 is now advanced by 2 CAD to 21° aTDC. Significantly, however, the stability limited line has shifted by nearly 13 degrees CAD to 24° aTDC, now only 3 CAD are available for combustion retard.
3. Under these conditions, the engine CR has increased to 12.0:1. The stability limited point remains the same at 24° aTDC, but the engine knock propensity increases from the increase in CR. Under these conditions, it is not possible to retard combustion phasing owing to the CoV limit. Therefore, load must be reduced. In this case, load is reduced to 15 bar BMEP and is now at the knock-stability limited load condition.
4. Reducing LP-EGR moves the stability limit back to CA50 = 35° aTDC permitting an increase in load back to the target 20 bar BMEP. Compared to case 1, however, the 10 degrees additional retard results in lower efficiency operation compared to the lower CR configuration.

A comparison of the CR 12.0:1 with LP-EGR configuration #2 to the baseline configuration #1 can be seen in Figure 19. There is a significant BSFC improvement below 12 bar BMEP, which is likely to yield reduced cycle CO_2 values over most drive-cycles. The low-speed, high-load operating condition is worse with the high-CR, although this condition was run without lean-scavenging so a direct comparison cannot be made. At higher loads and speeds, the need to retard CA50 ultimately leads to high BSFC.

A promising strategy to mitigate knock with high CRs is by utilizing early or late intake valve closing (EIVC or LIVC), commonly referred to as Miller- or Atkinson-cycle operation. Miller-cycle operation reduces the effective CR to reduce knock, while maintaining a high expansion ratio for efficiency benefits. The synergy between high CR and EIVC or LIVC has recently shown promise in the automotive industry but was not investigated in this work for two reasons:

1. The base engine valve train is set up for EIVC operation but only with significant valve-lift reduction. Reducing the valve lift reduces volumetric efficiency, placing a higher requirement for electrical over a wider area of the operating map. In this specific setup, the additional boost would be above the boost required for EGR dilution owing to the very low valve lift.
2. LIVC work would have required modified camshaft design, beyond the scope of this task.

In future work, we intend to investigate the potential of variable geometry turbine (VGT) hardware for combined Miller and EGR strategies.

Full-Load Comparison

In this section, full load data are presented and analyzed for the three configurations discussed in the previous sections. Figure 20 highlights combustion data and engine efficiency for the three configurations. All configurations met the target torque curve and therefore BSFC values can be directly compared.

The baseline configuration (black), as discussed previously, utilizes a lean scavenging calibration resulting in equivalence ratios below ϕ = 0.8 and O_2 concentrations in the tailpipe > 8%, far higher than the TWC operating window for NO_x reduction [28]. The BSFC for this baseline configuration (Euro V calibration) is comparable to the other configurations at low engine speeds. However, it is non-compliant with US standards. At the same low-speed conditions, 20% LP-EGR dilution is used instead of 20% lean dilution for the CR 10.5:1 with LP-EGR configuration (red) and, unsurprisingly, similar BSFC results can be seen. For the CR 12.0:1 configuration (blue), the engine had not reached the knock-stability limit at the lowest speeds owing to the low load target and BSFC values are therefore comparable. However, after 1500 rpm (17 bar, BMEP), LP-EGR is reduced and CA50 is significantly retarded, resulting in higher BSFC compared to the two CR 10.5:1 engine configurations.

Under the mid-speed conditions, the baseline-configured engine ran at stoichiometric tailpipe conditions. CA50 was retarded compared to the low CR LP-EGR configuration, owing to higher knock activity in the absence of LP-EGR. Nearly all the LP-EGR was removed from the high CR at the mid-speed condition. Additionally, CA50 was retarded compared to the other configurations owing to the increased knock propensity. Therefore, fuel enrichment was required, as eventually the 900 °C exhaust port temperature limit (930 °C pre-turbine) was reached. Beyond this point, any further power increase (load or speed increase) required enrichment to stay below the EGT threshold limit.

Under the high engine speed conditions, the baseline engine configuration required enrichment, and an increase in BSFC is seen compared to the CR 10.5:1 with LP-EGR configuration. This configuration remained stoichiometric at all engine speeds with a peak temperature of 891 °C reached at the 5000 rpm case. LP-EGR was reduced at the 5000 rpm point owing to the compressor-out temperature reaching a limit of 200 °C. The stock compressor was undersized for this application. Therefore, at the high engine speeds, with dilution, the compressor was operating near the choke limit where efficiency is poor, and high temperatures are observed during gas compression. At 4750 rpm, the non-EGR case and EGR case have identical combustion phasings, however the non-EGR case requires enrichment to stay below 900 °C port temperature limit (930 °C preturbine). The lower exhaust temperature highlights the lower combustion temperature benefit of the LP-EGR operation. At the final 5000 rpm point, the BSFC for the CR 10.5:1 condition with EGR is 21% lower compared to the CR 12.0:1 condition and 8.2% lower than the baseline configuration without EGR.

Premium vs Regular Fuel

Until recently, vehicle emission certification in the US used premium quality fuel with a high anti-knock index (AKI 93). Previous testing in this report was performed using a Tier 2 certification fuel with 93 AKI. Both EPA Tier 3 and California LEV III emissions standards are transitioning to the use of regular-grade

(approximately 87-88 AKI)[2] fuels blended with 10% ethanol and with a lower aromatic and carbon content for demonstrating compliance with criteria pollutant standards. Tier 3 and LEV III certification fuels are formulated to approximately reflect average fuel properties for "regular grade" gasoline in the U.S. and in California, respectively. Tier 2 certification fuel is still used for demonstrating compliance with U.S. light-duty GHG emissions standards. EPA analyses of the GHG effectiveness of light-duty vehicle engine technologies typically assume "regular grade" E10 gasoline will be the typical in-use fuel. In addition, any future hardware technology package must not be overly sensitive to fuel octane, as it would result in an unacceptable engine power de-rate if a consumer used regular fuel rather than premium.

Therefore, a short study to assess the effect of regular and premium fuels was performed. All testing in the following section was performed on the CR 10.5:1 with LP-EGR configuration. First, the engine was run under 11 part-load conditions with a regular fuel, and the efficiency was compared to the premium fuel data previously taken. Then, a full-load curve was run to ensure that the engine could meet the full-load target achieved by the premium fuel.

All part-load points were run at the optimal combustion phasing of approximately CA50 = 8° aTDC. Results for the part-load conditions can be seen in Figure 21. Efficiency is shown as BTE rather than BSFC owing to the ethanol content of the regular fuel. Lower heating values (LHVs) for the two fuels were measured at Southwest Research Institute (SwRI) according to ASTM D240 standards.

For most cases, the premium fuel appeared to have higher efficiency, with the average difference between the two fuels approximately 0.6% in favor of the premium fuel. The 0-50 CAD burn duration is shorter for the regular fuel (as can be deduced from Figure 22), likely owing to the ethanol content. Faster combustion, with the same combustion phasing, should yield higher efficiency. The LHV measurement is ±1% and therefore, the average difference is well within the limit of the LHV resolution. The result suggests that performance between the two fuels under part-load conditions is essentially the same.

Two full load curves were generated during this fuel study using the regular fuel. The difference in the two curves was the way that back pressure was set. For one test, back pressure was set to MAP. For the next test, back pressure was set to simulated values. Simulation was performed using a 0d/1d combustion and gas dynamics model, Gamma Technologies Inc., GT-Power, to model the back pressure of a single-stage variable turbine geometry turbocharger. A further discussion of the modeling process can be seen in [21]. The modeling exercise was necessary to provide accurate back pressure values while using the electrically driven supercharger. Results from the two tests can be seen in Figure 23.

When back pressure was matched to manifold pressure, the engine was unable to meet the full load target at low engine speeds when utilizing the same LP-EGR rate as run on the premium fuel. Engine load could not be increased because the engine reached the knock-stability limit and remained 4 bar BMEP short of the target 20 bar BMEP at 1750-2000 rpm. For the second test, the pre-turbine pressure was set to values simulated with GT-Power. The back-pressure simulated was, on average, 40 kPa lower than using the matched MAP method between 1500 rpm and 2500 rpm. VNT back pressure is typically

[2] Manufacturers may request higher AKI LEV III fuels be used for certification and compliance testing if such fuel is required by the manufacturer during in-use vehicle operation.

observed to be lower than wastegated turbochargers [18,19,20]. A lower back pressure reduces hot trapped residual content. The reduction of hot residuals lowers the in-cylinder gas temperature, avoiding knock. CA50 could therefore be advanced The CA50 advance increases engine load through better air utilization and also moved the engine away from the knock-stability limited operating boundary. With the lower back pressure, it was possible to achieve the target full-load curve albeit with reduced efficiency compared to the Tier 2 premium fuel case.

There are differences between Tier 2 and LEV III fuels which directly affect the net CO2 production independent of efficiency. The lower aromatic content of the Tier 3 and LEV III certification fuels results in a lower carbon content, thereby slightly reducing CO2 emissions relative to Tier 2 fuel over the regulatory drive cycles for GHG compliance as can be seen in [29].

Drive Cycle Analysis

ALPHA input fuel maps were created [25] to represent fuel consumption for all three of the PSA engine configurations (OEM PSA, 12.0:1 CR with LP-EGR, and 10.5:1 CR with LP-EGR). ALPHA drive cycle simulations were then conducted for each engine configuration to estimate the combined energy-weighted, two-cycle (EPA city and highway) GHG emissions expressed as g/mi CO2. Table 3 contains a summary of the results of this set of simulations for an example model year (MY) 2016 mid-sized light-duty passenger car weighing 3510 pounds and equipped with a conventional 6-speed automatic transmission. Identical test weights and road load coefficients were used for the simulation runs with each engine (Table 3). The descriptions of the engines in Table 3 shows slight displacement differences for each PSA engine needed to power this example vehicle while maintaining performance equivalent to the base vehicle. Engine scaling to maintain equivalent performance for ALPHA vehicle simulations has been previously described [25]. Note that the ALPHA results do not include the addition of air conditioning or off-cycle credits and do not include road load reductions or transmission efficiency improvements that are expected in the post-MY2017 timeframe.

The ALPHA drive cycle modeling results estimate that replacing the baseline PSA engine with the 10.5 CR LP-EGR engine in the example mid-size vehicle would reduce CO_2 emissions by 3.2%. When the 10.5 CR LP-EGR engine is replaced with the 12 CR LP-EGR engine, the ALPHA results show that the CO2 emissions would be reduced by an additional 2.5%.

Summary/Conclusions

Based on engine testing of three different engine configurations, and testing the impact of two different fuels, the following conclusions can be reached:

- The addition of LP-EGR resulted in efficiency improvements across the engine operating map at a 10.5:1 CR. The largest efficiency improvements were observed at high load conditions where the knock mitigation benefit of LP-EGR permitted CA50 advance and therefore efficiency improvement. Peak BTE increased by 4.5% compared to the non-EGR case. At lower loads, a small efficiency improvement from improved heat transfer was observed.
- For the 10.5:1 CR configuration at full load, the addition of LP-EGR enabled the engine to run under stoichiometric conditions up to the peak-power condition with advanced CA50 timing compared to the other two configurations. Therefore, the efficiency of the LP-EGR 10.5:1 CR

case was superior to both the baseline case and the high CR at almost all full-load points. LP-EGR was reduced in the peak-power case to avoid high compressor-out temperatures.

- The stock boost device was unable to meet the required torque curve when LP-EGR was utilized. The relatively large compressor surged under the high-pressure ratio, low flow condition at low-engine speed, high-load conditions. An electronic supercharger, post-compressor, was used to supply additional boost. A detailed simulation study to assess the potential of a single variable geometry turbine on this engine platform is discussed in [21].
- The addition of LP-EGR reduces combustion stability. Therefore, the knock-limited CA50 and stability-limited CA50 converge at a lower engine load and can limit performance as was seen for the CR 12.0:1 configuration. Removing EGR is a possible solution as it enables further CA50 retard. However, efficiency is impacted, especially at higher loads where the enrichment requirement increases.
- Increasing CR from 10.5:1 to 12:1 improved engine efficiency at loads below 12 bar BMEP. The improvement was mainly attributed to the higher expansion ratio.
- At higher engine loads (>16 bar BMEP), LP-EGR had to be reduced with the CR 12.0:1 configuration to achieve the target load because of combustion phasing retard causing combustion to become unstable (CoV IMEP >3%).
- To be considered a viable option for manufacturers, the LP-EGR technology must not be limited by fuel octane. Testing of a high octane and low octane fuel identified that it was possible to achieve the target full-load performance with the low octane fuel. The area of interest was at the knock-limited low-speed, high-load region of the map. Although the engine could meet the performance targets, efficiency was reduced compared to the high-octane fuel test.
- Switching from the Tier 2 to a LEV III fuel resulted in a CO_2 reduction at the speed and load conditions experienced on regulatory drive cycles. The reduction is due to a lower aromatic content of the LEV III fuel which increases the hydrogen to carbon ratio.
- ALPHA drive cycle modeling was used to predict the effect of LP-EGR and CR on CO_2 produced over a combined EPA city and highway drive cycles. CO_2 was reduced by 3.2% when adding LP-EGR and a further 2.5% by increasing the CR. It is likely that these results would be lower in a real-world application as EGR is avoided under cold conditions to avoid condensation problems.

References

1. Diana, S., Giglio, V., Iorio, B., and Police, G., “Evaluation of the Effect of EGR on Engine Knock,” SAE Technical Paper 982479, 1998, doi:10.4271/982479.

2. U.S. EPA Office of Transportation and Air Quality, “Regulatory Announcement,” Document Number EPA-420-F-12-051, August 2012.

3. U.S. EPA Office of Transportation and Air Quality, “Regulatory Announcement,” Document Number EPA-420-F-14-009, March 2014.

4. Alger, T., Gingrich J., Mangold B., and Roberts C., Cooled EGR for Fuel Economy and Emissions Improvement in Gasoline Engines, in JSAE Paper 447-20105013, J.P. 447-20105013, Editor. 2010.

5. Roberts, P. and Sheppard, C., “The Influence of Residual Gas NO Content on Knock Onset of Iso-Octane, PRF, TRF and ULG Mixtures in SI Engines,” SAE Int. J. Engines 6(4):2028-2043, 2013.

6. Alger, T., Mangold, B., Roberts, C., and Gingrich, J., “The Interaction of Fuel Anti-Knock Index and Cooled EGR on Engine Performance and Efficiency,” SAE Int. J. Engines 5(3):1229-1241, 2012.

7. Szybist, J., Wagnon, S., Splitter, D., Pitz, W. et al., “The Reduced Effectiveness of EGR to Mitigate Knock at High Loads in Boosted SI Engines,” SAE Int. J. Engines 10(5):2305-2318, 2017.

8. Sjoberg, M., Dec, J., and Hwang, W., “Thermodynamic and Chemical Effects of EGR and Its Constituents on HCCI Autoignition,” SAE Technical Paper 2007-01-0207, 2017, doi:10.4271/2007-01-0207.

9. Cairns, A., Blaxill, H., and Irlam, G., “Exhaust Gas Recirculation for Improved Part and Full Load Fuel Economy in a Turbocharged Gasoline Engine,” SAE Technical Paper 2006-01-0047, 2006, doi:10.4271/2006-01-0047.

10. Duchaussoy, Y., Lefebvre, A., and Bonetto, R., “Dilution Interest on Turbocharged SI Engine Combustion,” SAE Technical Paper 2003-01- 0629, 2003, doi:10.4271/2003-01-0629.

11. Grandin, B., Ångström, H., Stålhammar, P., and Olofsson, E., “Knock Suppression in a Turbocharged SI Engine by Using Cooled EGR,” SAE Technical Paper 982476, 1998, doi:10.4271/982476.

12. Alger, T., Gingrich, J., Khalek, I., and Mangold, B., “The Role of EGR in PM Emissions from Gasoline Engines,” SAE Int. J. Fuels Lubr. 3(1):85-98, 2010, doi:10.4271/2010-01-0353.

13. Hedge, M., Weber, P., Gingrich, J., Alger, T. et al., “Effect of EGR on Particle Emissions from a GDI Engine,” SAE Int. J. Engines 4(1):650-666, 2011, doi:10.4271/2011-01-0636.

14. Potteau, S., Lutz, P., Leroux, S., Moroz, S. et al., “Cooled EGR for a Turbo SI Engine to Reduce Knocking and Fuel Consumption,” SAE Technical Paper 2007-01-3978, 2007, doi:10.4271/2007-01-3978.

15. Alger, T., Gukelberger, R., Gingrich, J., and Mangold, B., “The Impact of Cooled EGR on Peak Cylinder Pressure in a Turbocharged, Spark Ignited Engine,” SAE Int. J. Engines 8(2), 2015, doi:10.4271/2015-01-0744.

16. Aiyoshizawa, E. and Hori, K., “The New Nissan High Efficient 4-Cylinder 1.6 L GDI Turbocharged Engine with Low Pressure EGR - Evolution for Lower Fuel Consumption Combined with High Output Performance,” 35. Internationales Wiener Motoren Symposium, 2014.

17. Sasaki, Y., Adachi, S., Nakata, K., Tanei, K., et al., “The New Toyota 1.0 L L3 ESTEC Gasoline Engine,” 35. Internationales Wiener Motorensymposium, 2014.

18. Eichler, F., Demmelbauer-Ebner, W., Theobald, J., and Stiebels, B., "The New EA211 TSI evo from Volkswagen," in *International Vienna Motor Symposium*, 2016.

19. Claus, G., Kluin, M., Hermann, I., and Koenigstein, A., "980 °C Gasoline Variable Turbine Geometry - The Affordable Upcoming Technology for High-Volume Efficient Engines," *26th Aachen Colloquium Automobile and Engine Technology 2017*, October 2017, 469-87.

20. Bontemps, N., Roux, J.-S., Jeckel, D., and Schlosshauer, A., “VNT Turbocharger for Gasoline "Miller" Engines,” *International Conference and Exhibition SIA Powertrain Versailles* 07:2017, 2017, June.

21. Robertson, D., Conway, G., Chadwell C., et al, “Predictive GT-Power Simulation for VNT matching on a 1.6 L Turbocharged GDI Engine”, Submitted for 2018 SAE World Congress, SAE 2018-01-0161, 2018.

22. U.S. EPA. Proposed Determination on the Appropriateness of the Model Year 2022-2025 Light-Duty Vehicle Greenhouse Gas Emissions Standards under the Midterm Evaluation: Technical Support Document. § 2.2 State of Technology and Advancements since the 2012 Final Rule. Document Number EPA-420-R-16-021, November 2016.

23. Lee, B., Lee, S., Cherry, J., Neam, A. et al., “Development of Advanced Light-Duty Powertrain and Hybrid Analysis Tool (ALPHA),” SAE Technical Paper 2013-01-0808, 2013, doi:10.4271/2013-01-0808.

24. Newman, K., Kargul, J., and Barba, D., “Benchmarking and Modeling of a Conventional Mid-Size Car Using ALPHA,” SAE Technical Paper 2015-01-1140, 2015, doi:10.4271/2015-01-1140.

25. Dekraker, P., Kargul, J., Moskalik, A., Newman, K. et al., “Fleet-Level Modeling of Real World Factors Influencing Greenhouse Gas Emission Simulation in ALPHA,” *SAE Int. J. Fuels Lubr.* 10(1):217-235, 2017 https://doi.org/10.4271/2017-01-0899.

26. Roth, D., Keller, P., and Becker, M., “Requirements of External EGR Systems for Dual Cam Phaser Turbo GDI Engines,” SAE Technical Paper 2010-01-0588, doi:10.4271/2010-01-058.

27. Heywood, J.B., “Internal Combustion Engine Fundamentals,” In: *Ch.5 - Ideal Models of Engine Cycles*. (McGraw Hill, Inc., 1988).

28. Heck, R.M., Farrauto, R.J., Gulati, S.T. “*Catalytic Air Pollution Control: Commercial Technology*, Third Edition.” Ch. 6 - Automotive Catalyst. Wiley Publ., ISBN: 978-1-118-39771-8, 2012.

29. U.S. EPA. Proposed Determination on the Appropriateness of the Model Year 2022-2025 Light-Duty Vehicle Greenhouse Gas Emissions Standards under the Midterm Evaluation, Technical Support Document. §2.3.4.1.9.1 -Effectiveness Data Used and Basis for Assumptions (Table 2-71). Document Number EPA-420-R-16-021, November 2016.

Acknowledgments

Work by SwRI presented within this paper was conducted under contract to the U.S. EPA, Contract Number EP-C-15-006.

Disclaimer

The views expressed in this publication are those of the authors and do not necessarily represent the views or policies of the U.S. Environmental Protection Agency.

Definitions/Abbreviations

aTDC - After top dead center

BDC - Bottom dead center

BMEP - Brake mean effective pressure

BSFC - Brake specific fuel consumption

BTE - Brake thermal efficiency

bTDC - Before top dead center

CA - Crank angle

CAD - Crank angle degrees

CO - Carbon monoxide

CO2 - Carbon dioxide

CoV - Coefficient of variance

CR - Compression ratio

CVVL - Continuously variable valve lift

DCI - Dual coil ignition

DI - Direct injection

EPA - U.S. Environmental Protection Agency

EGR - Exhaust gas recirculation

EGT - Exhaust gas temperature

EIVC - Early intake valve closing

FTP - Federal Test Procedure

GDI - Gasoline direct injection

GHG - Green House Gas

HC - Hydrocarbon

IMEP - Indicated mean effective pressure

KLSA - Knock limited spark advance

LHV - Lower heating value

LIVC - Late intake valve closing

LP - Low-pressure

MAP - Manifold air pressure

MBT - Minimum spark advance for best torque

NEDC - New European drive cycle

NOx - Oxides of nitrogen

NMOG - non-Methane organic gases

OEM - Original equipment manufacturer

PID - Proportional-integral-derivative

PM - Particulate Matter

RDE - Real driving emissions

RON - Research octane number

SA - Spark advance

SI - Spark ignited

SOI - Start of injection

SwRI - Southwest Research Institute

TDC - Top dead center

TWC - Three-way catalyst

VGT - Variable geometry turbine

VNT - Variable nozzle turbine

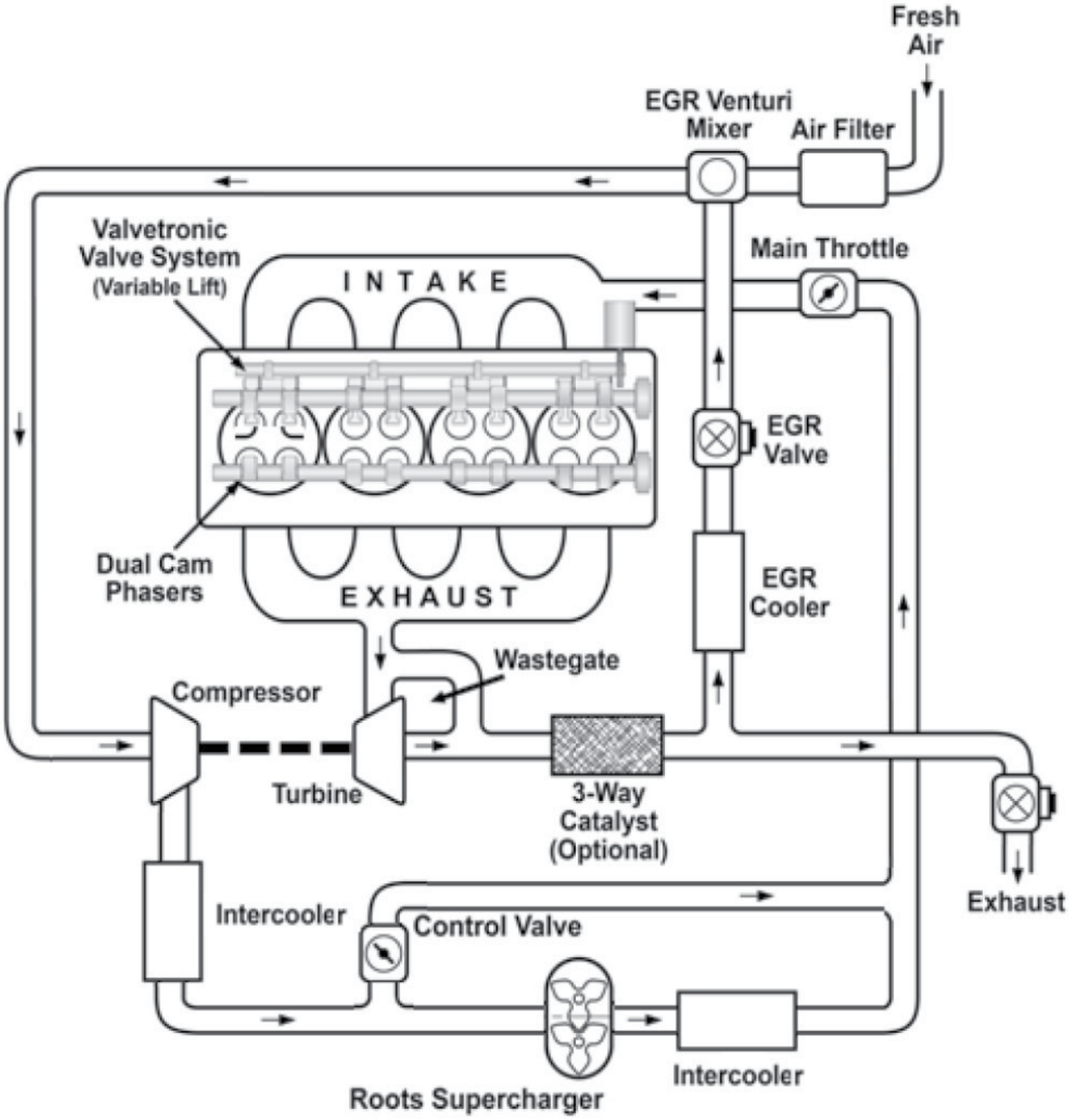

Figure 1 Schematic of engine configuration in test-cell

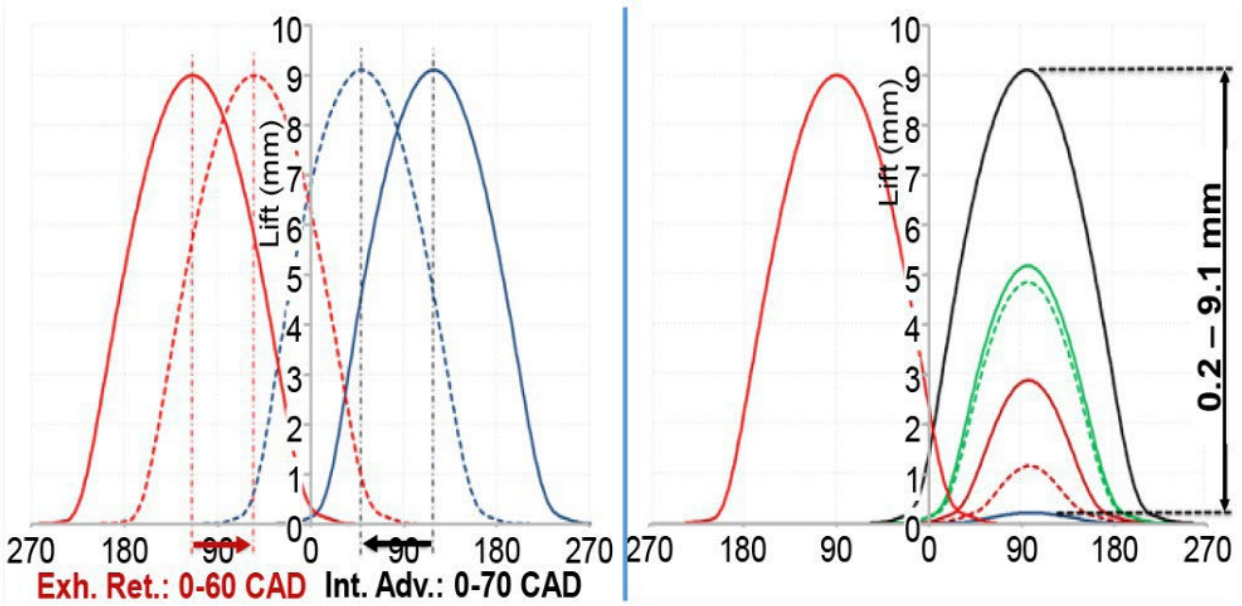

Figure 2 CVVL timing and lift profiles

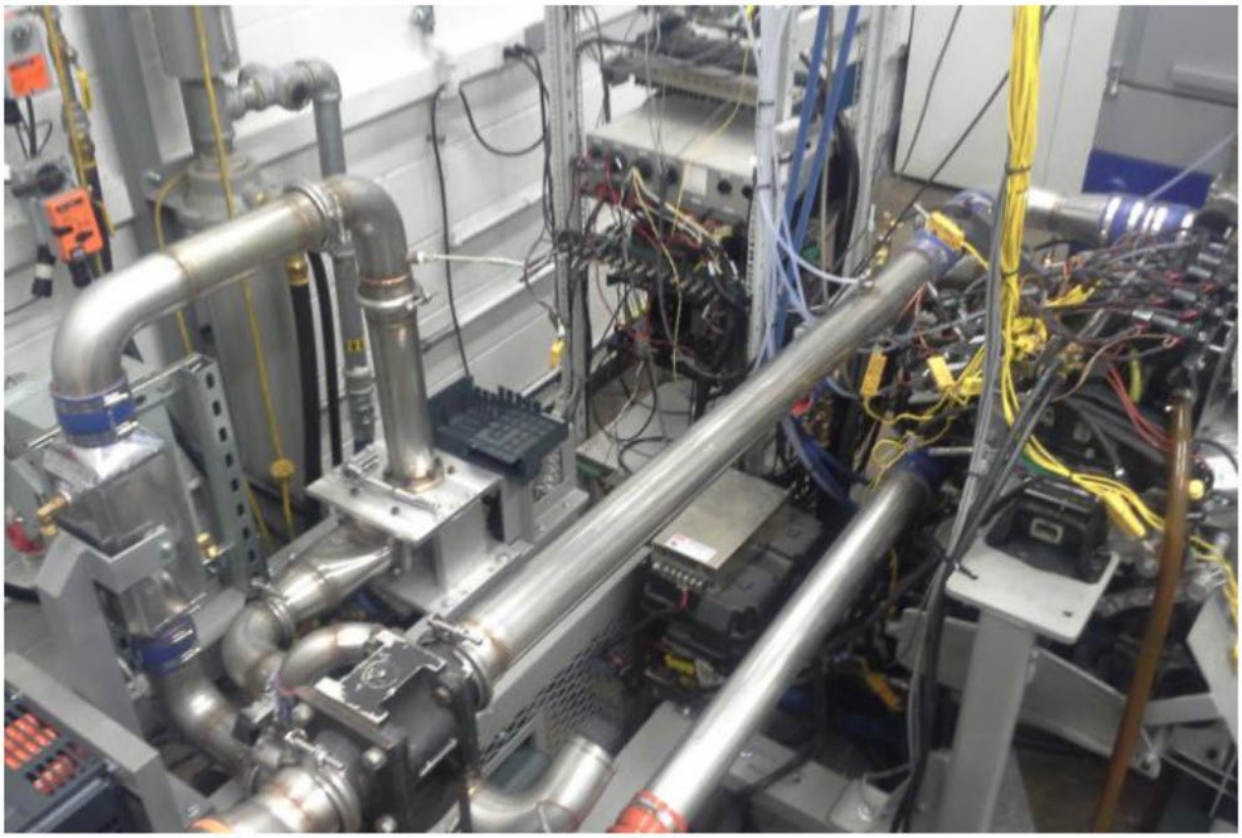

Figure 3 Engine test-cell installation at Southwest Research Institute Facility

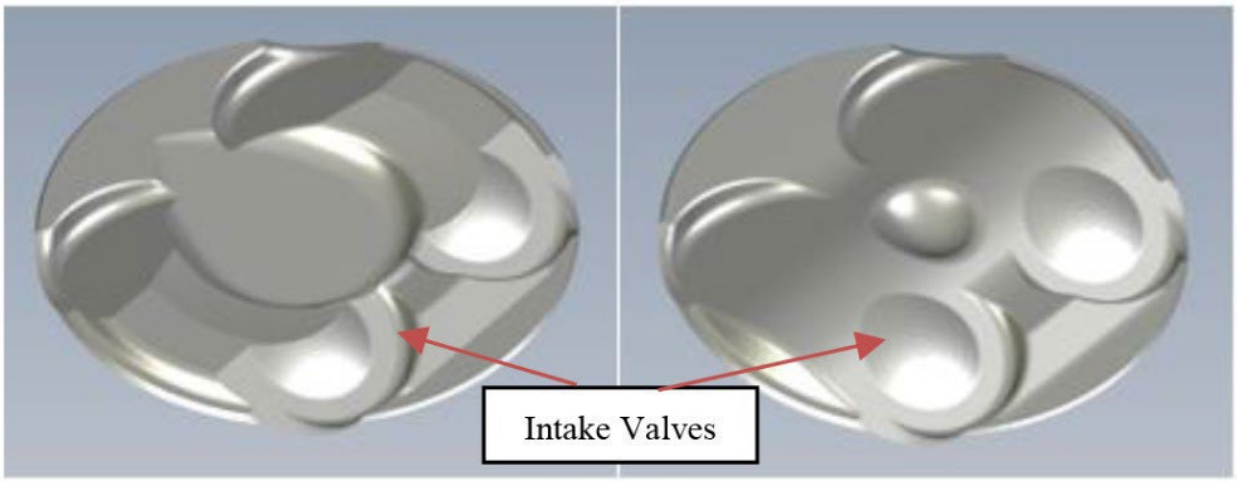

Figure 4 CR 10.5:1 (left) and CR 12.0:1 (right) piston geometries

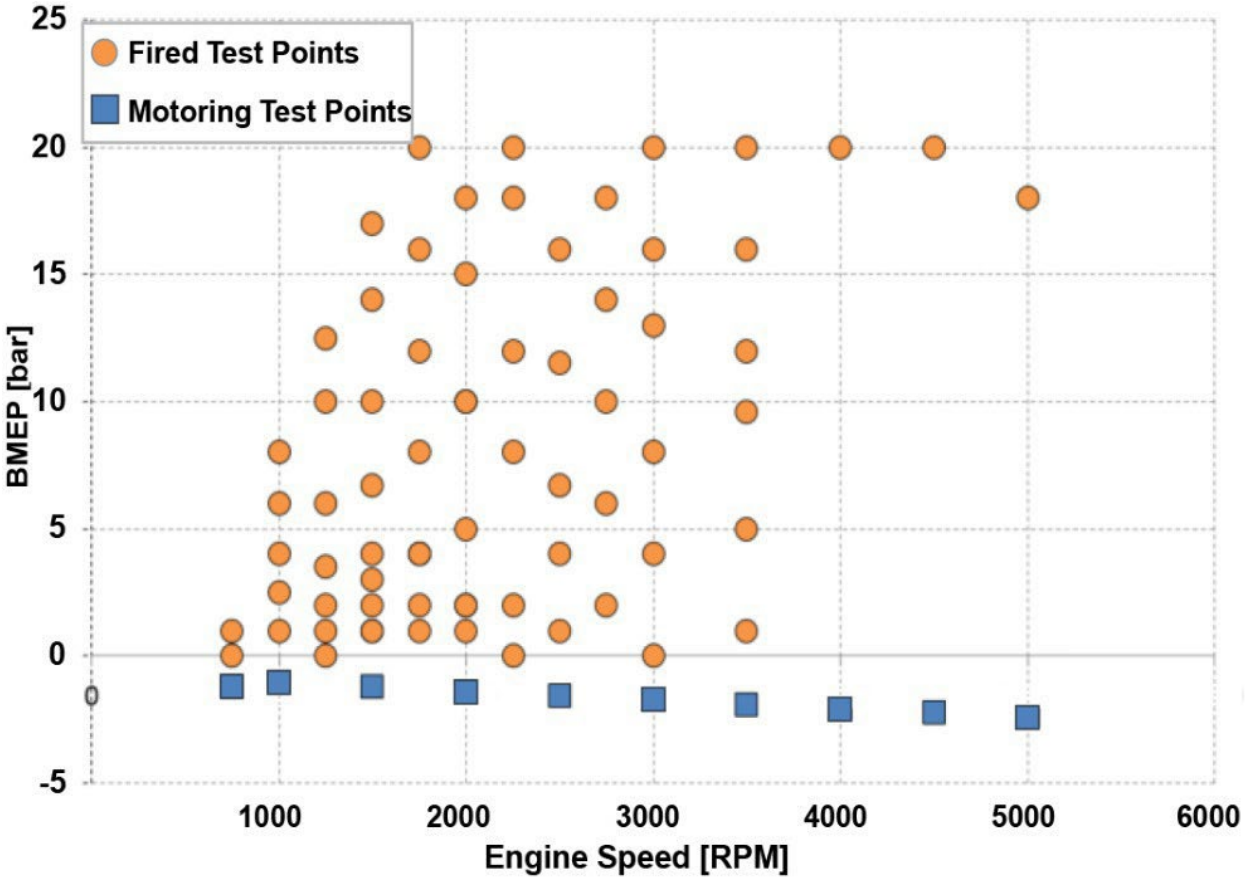

Figure 5 Speed-load operating points for the three engine configurations

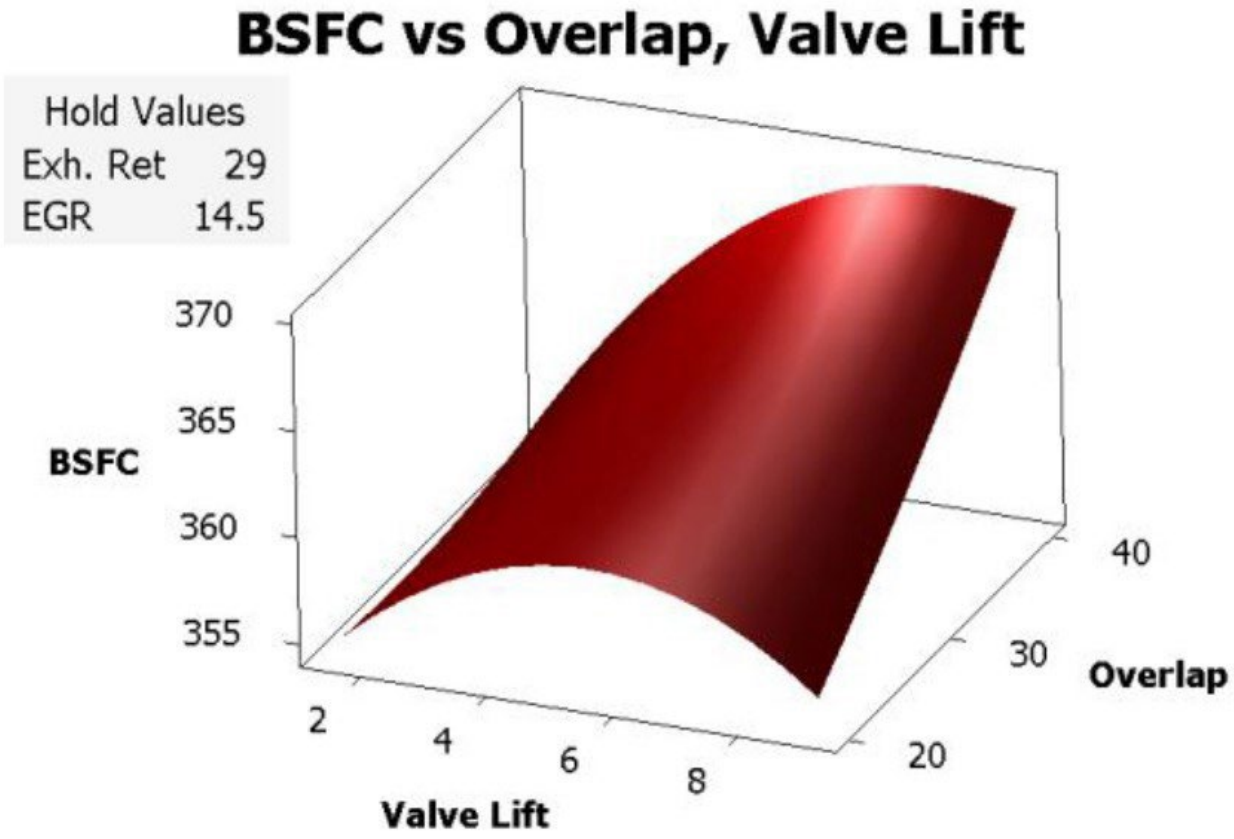

Figure 6 Response surface created from Box-Behnken DoE approach. Example surface plot at 2000 rpm 2 bar BMEP

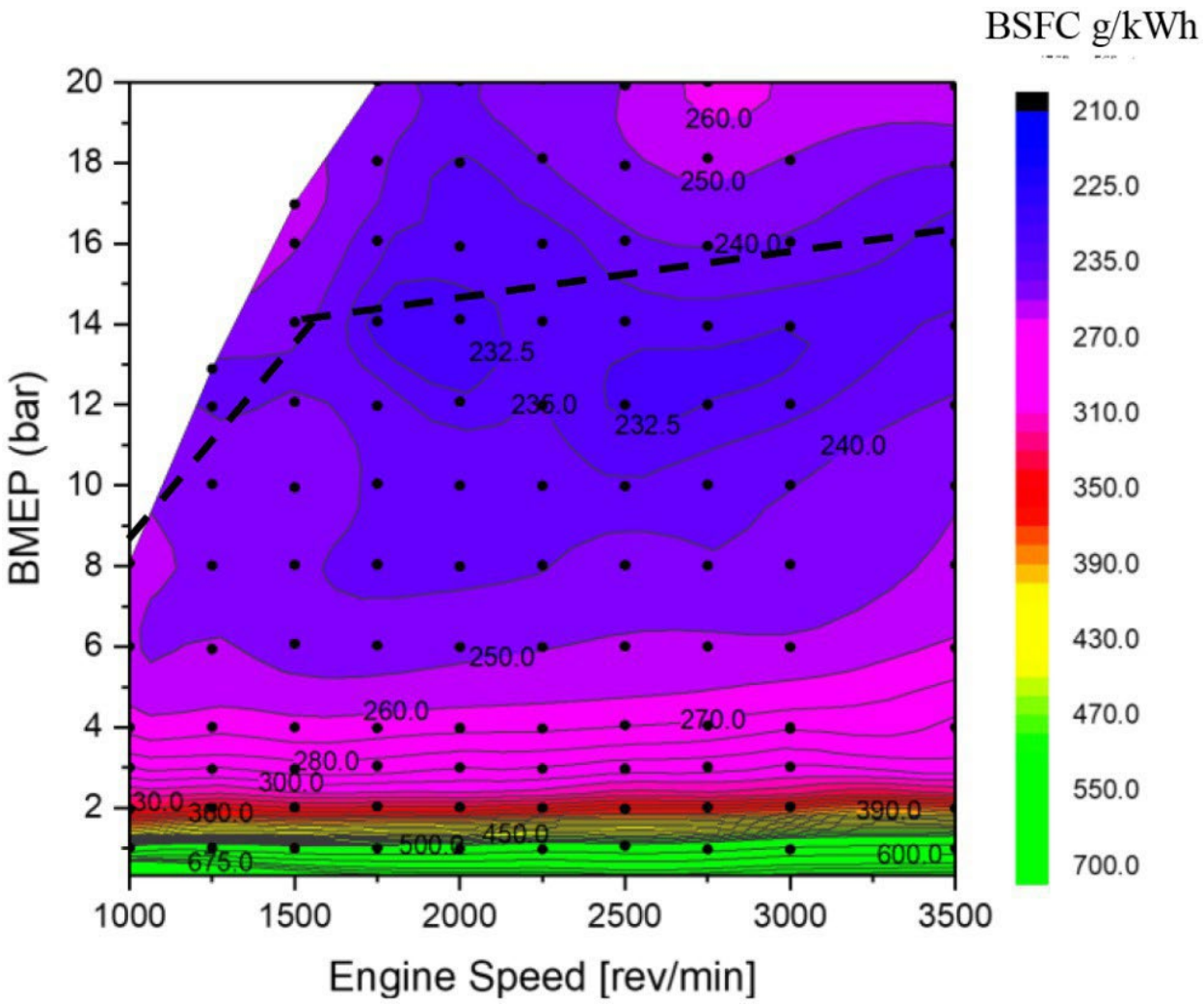

Figure 7 BSFC map for the baseline engine configuration with 10.5:1 CR and no external LP-EGR (Configuration 1). Maximum load at MBT timing identified by dashed black line.

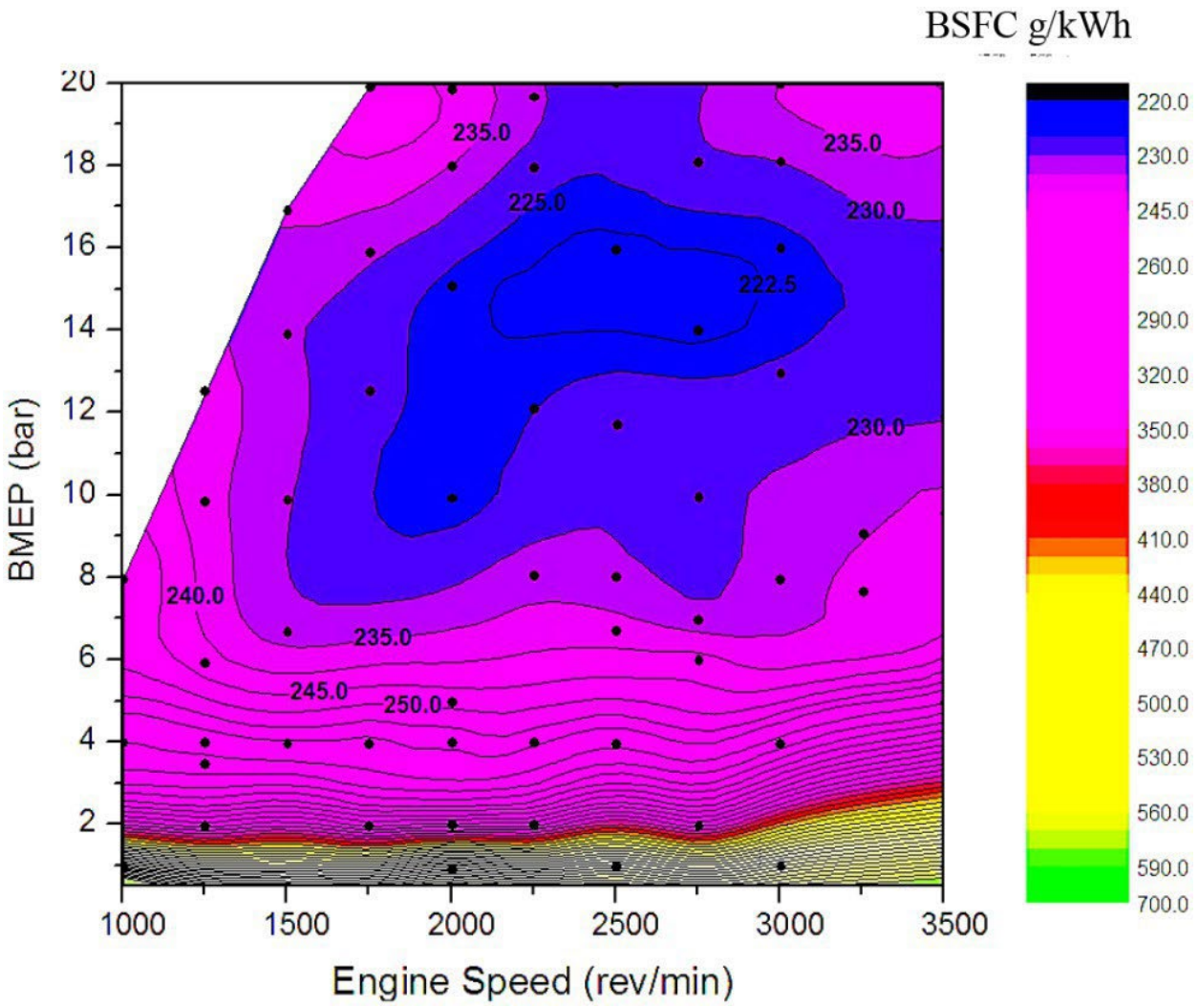

Figure 8 BSFC map for the 10.5:1 CR piston and external LP-EGR configuration (Configuration 2).

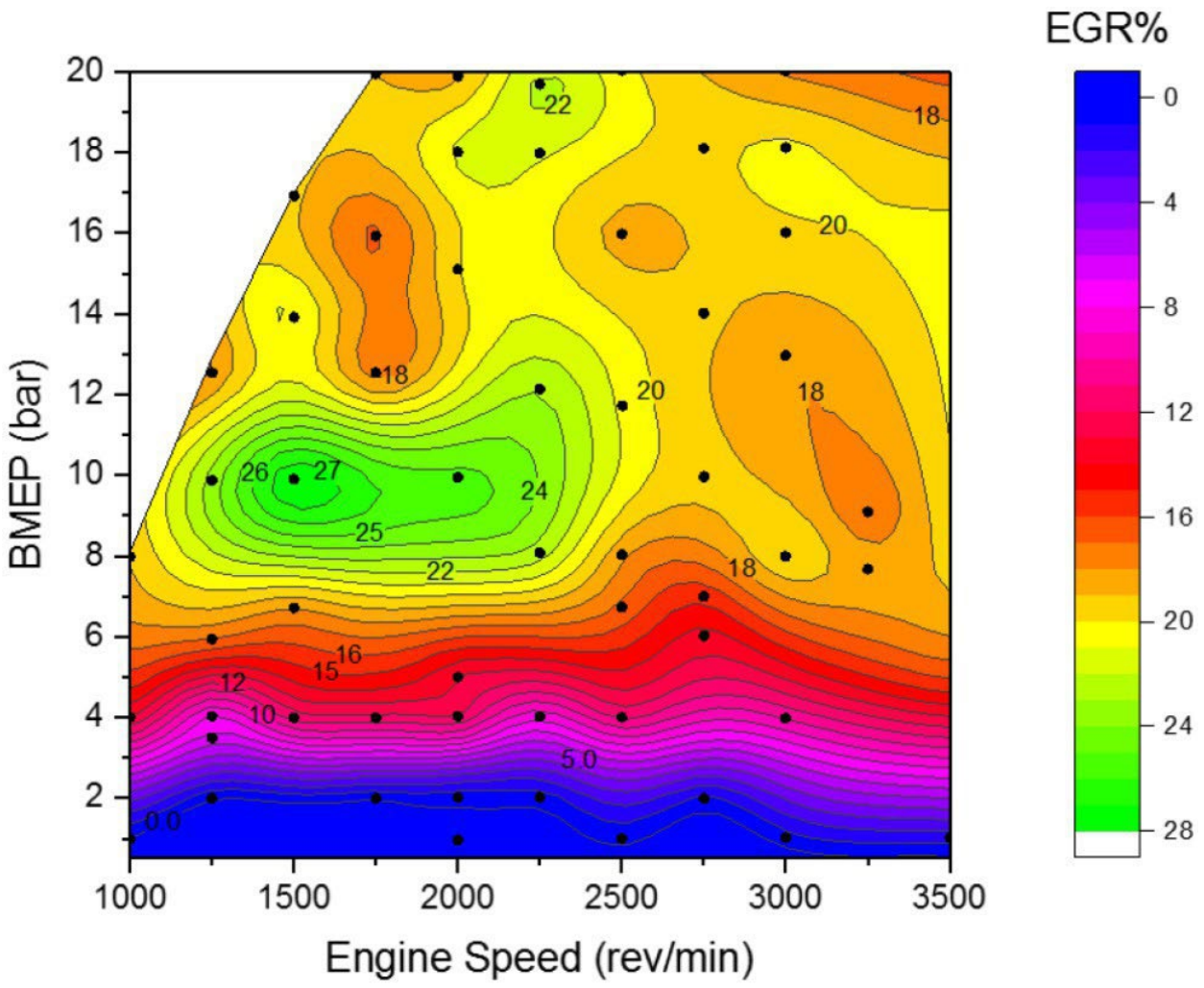

Figure 9 EGR rate map for the 10.5:1 CR piston and external LP-EGR configuration.

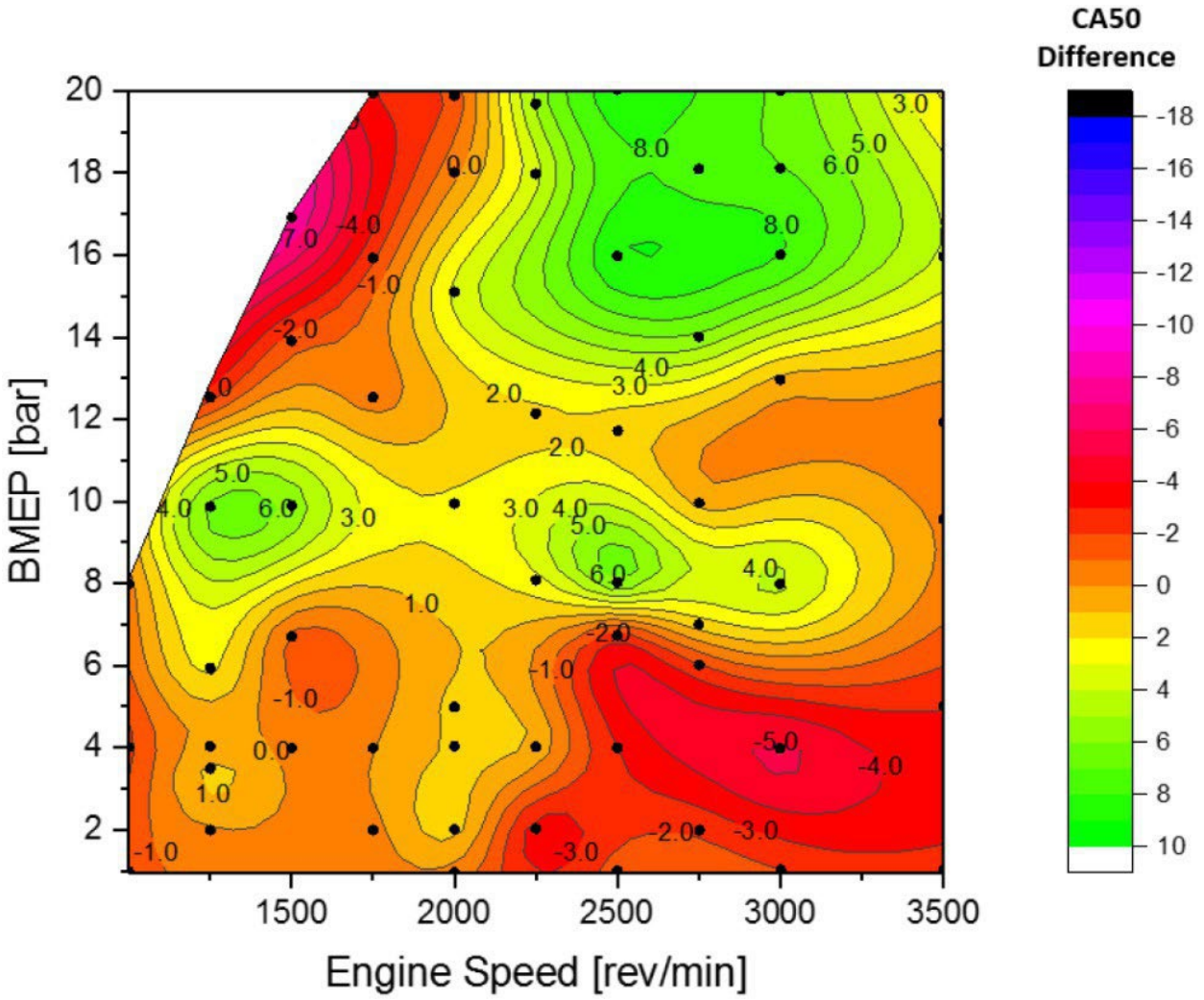

Figure 10 CA50 comparison map between the non-EGR and LP-EGR configurations. Positive values indicate earlier combustion phasing for the LP-EGR configuration

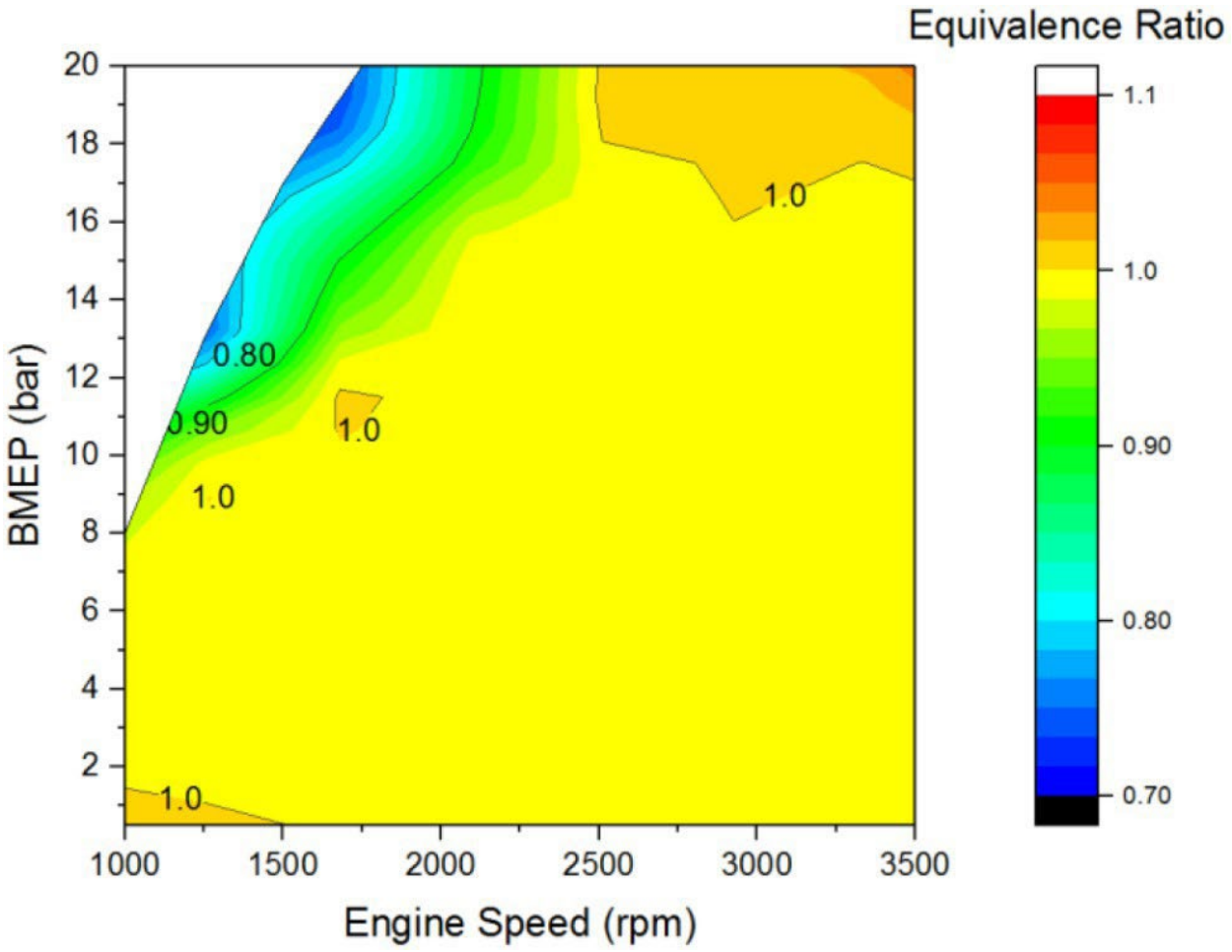

Figure 11 Baseline engine configuration equivalence ration contour for the CR 10.5:1 no-EGR figuration utilizing a typical lean-scavenging strategy

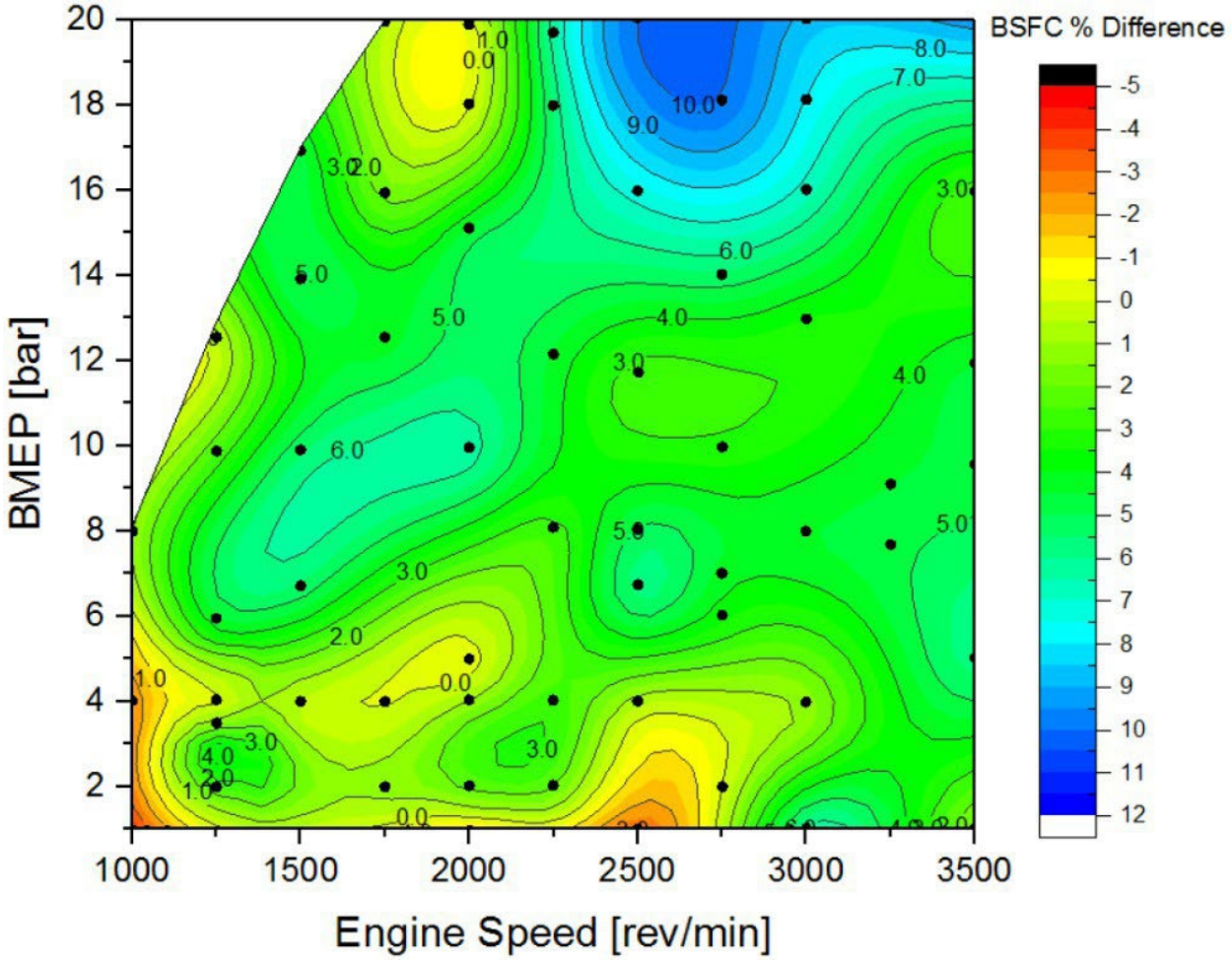

Figure 12 BSFC comparison map between the non-EGR and LP-EGR configurations. Positive values indicate a benefit for LP-EGR.

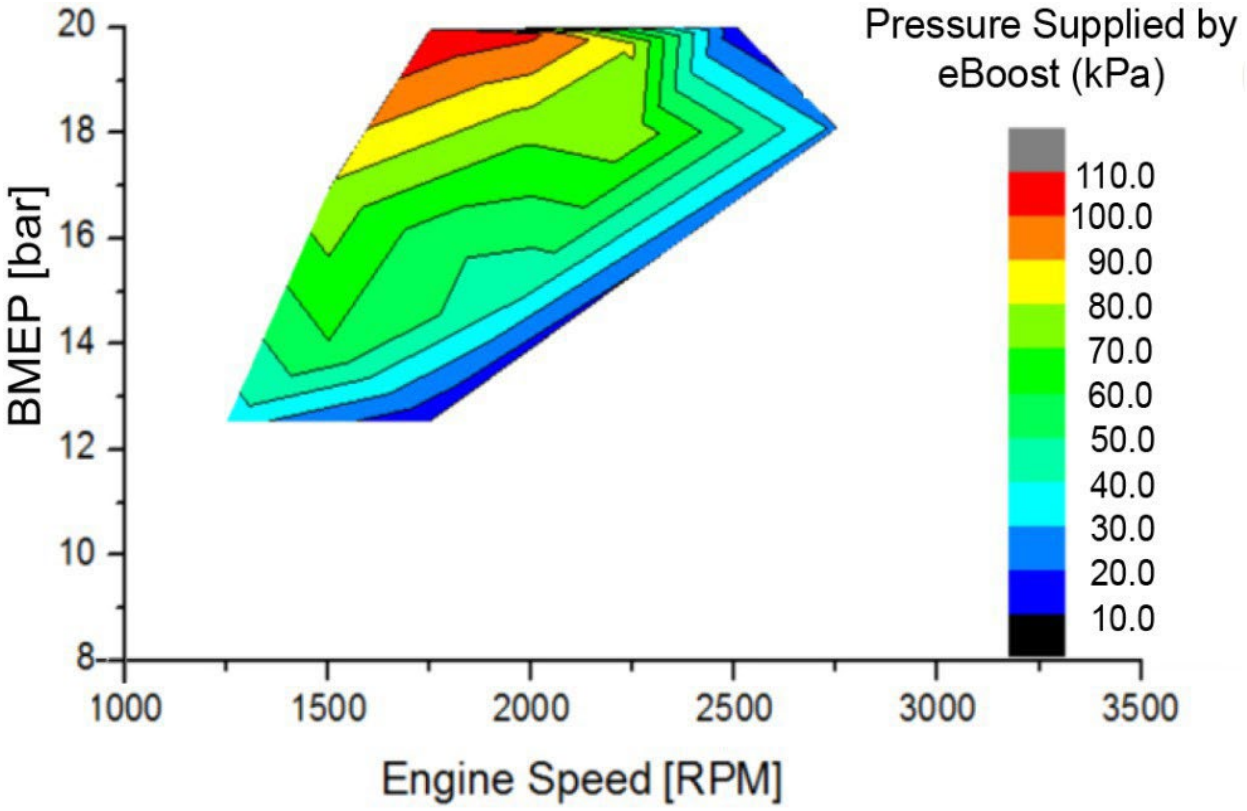

Figure 13 Pressure (gauge) supplied by supercharger.

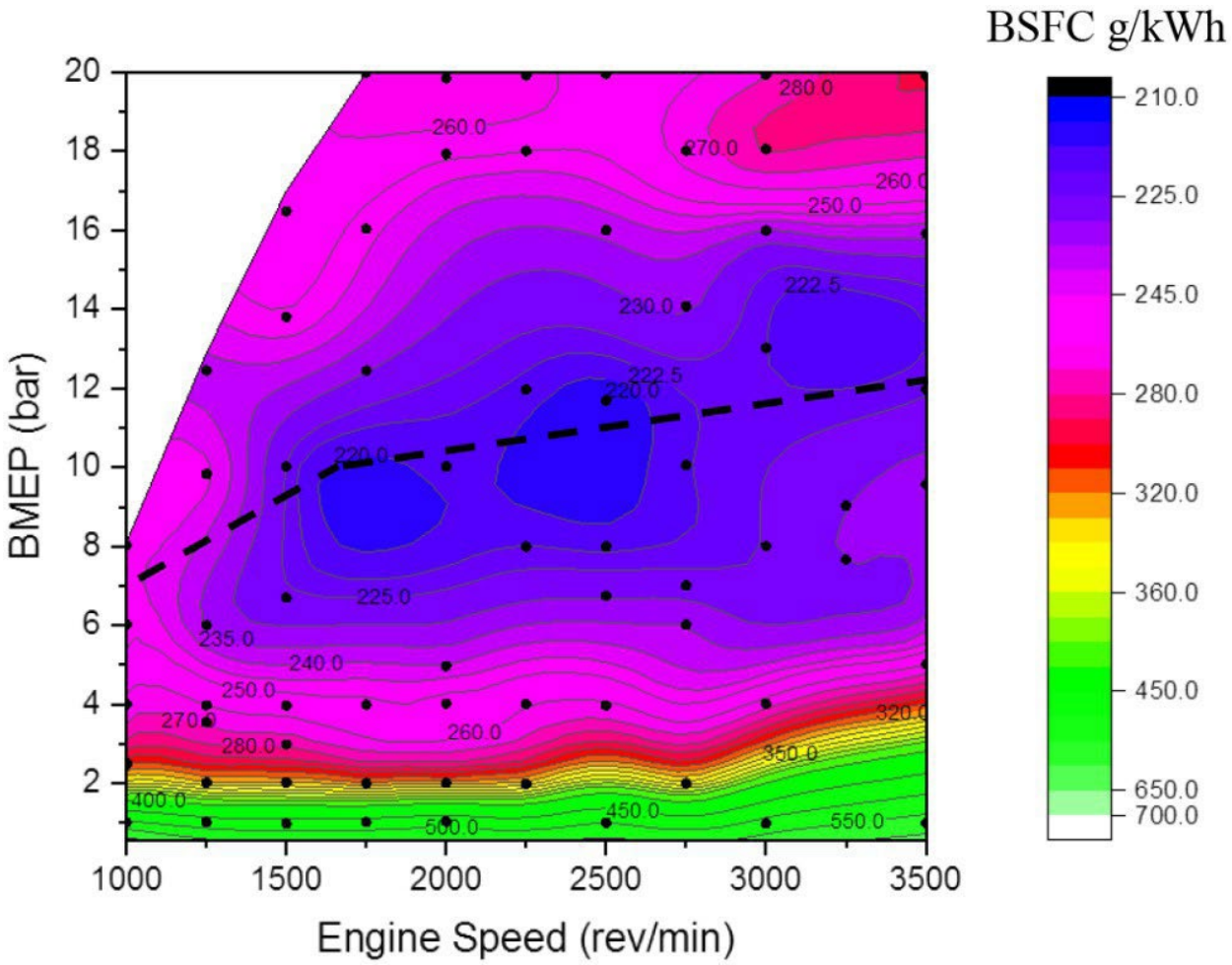

Figure 14 BSFC map for the 12.0:1 CR piston and external LP-EGR configuration (Configuration 3). The maximum load at MBT timing is represented by the dashed black line.

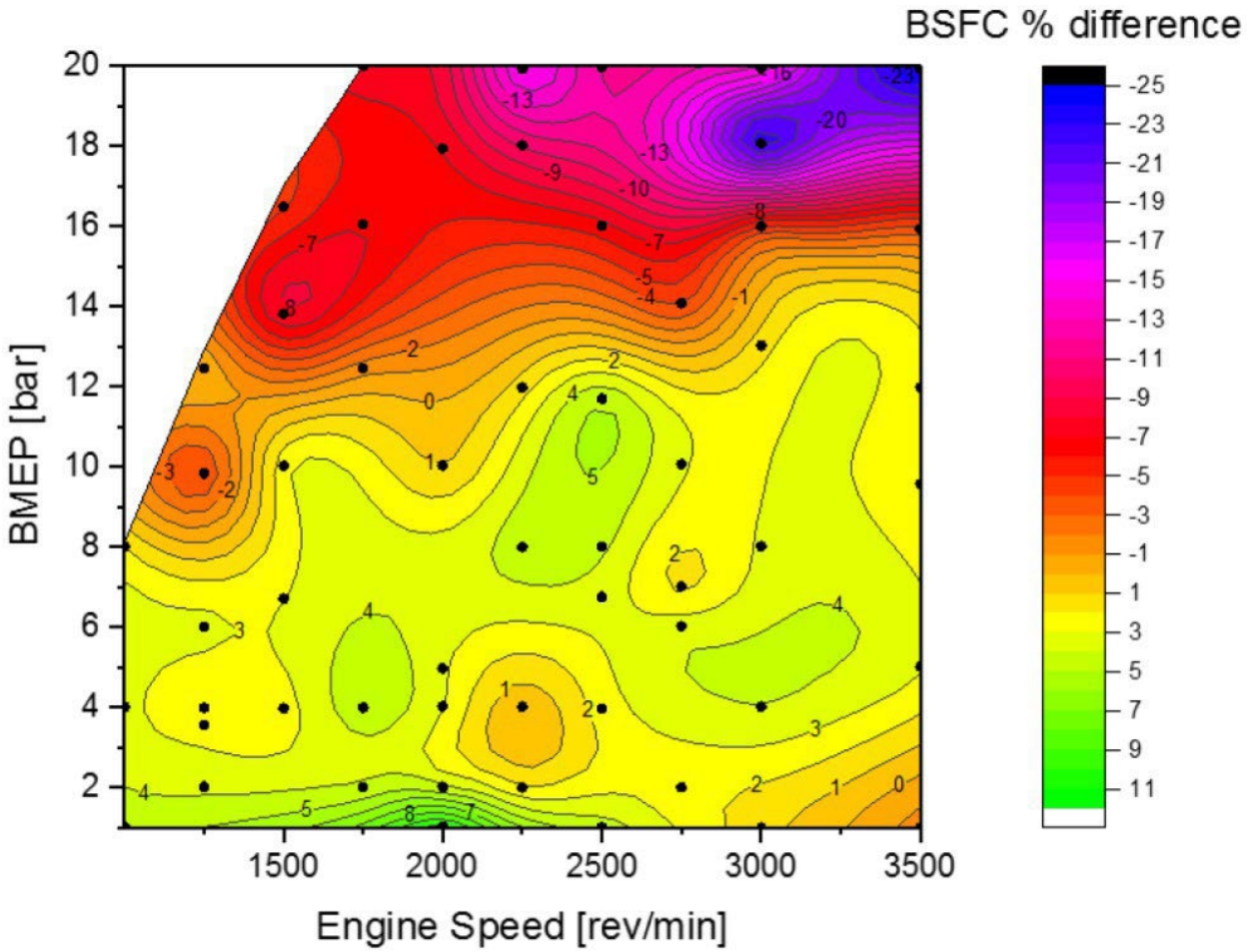

Figure 15 BSFC comparison map between CR 12.0:1 and CR 10.5:1 with LP-EGR. Positive values indicate BSFC is lower for the CR 12.0:1 case.

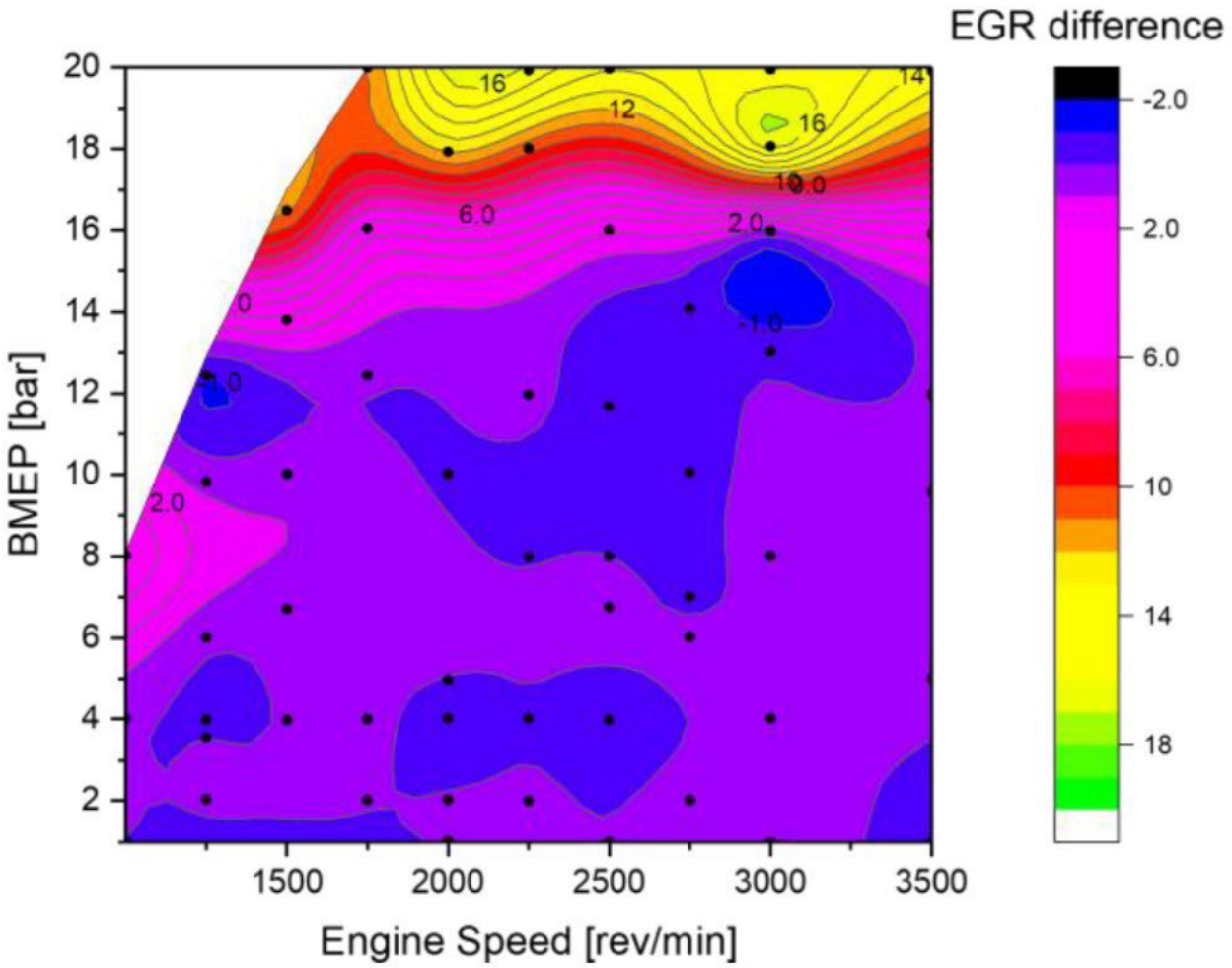

Figure 16 EGR rate map for the 12.0:1 CR piston and external LP-EGR configuration.

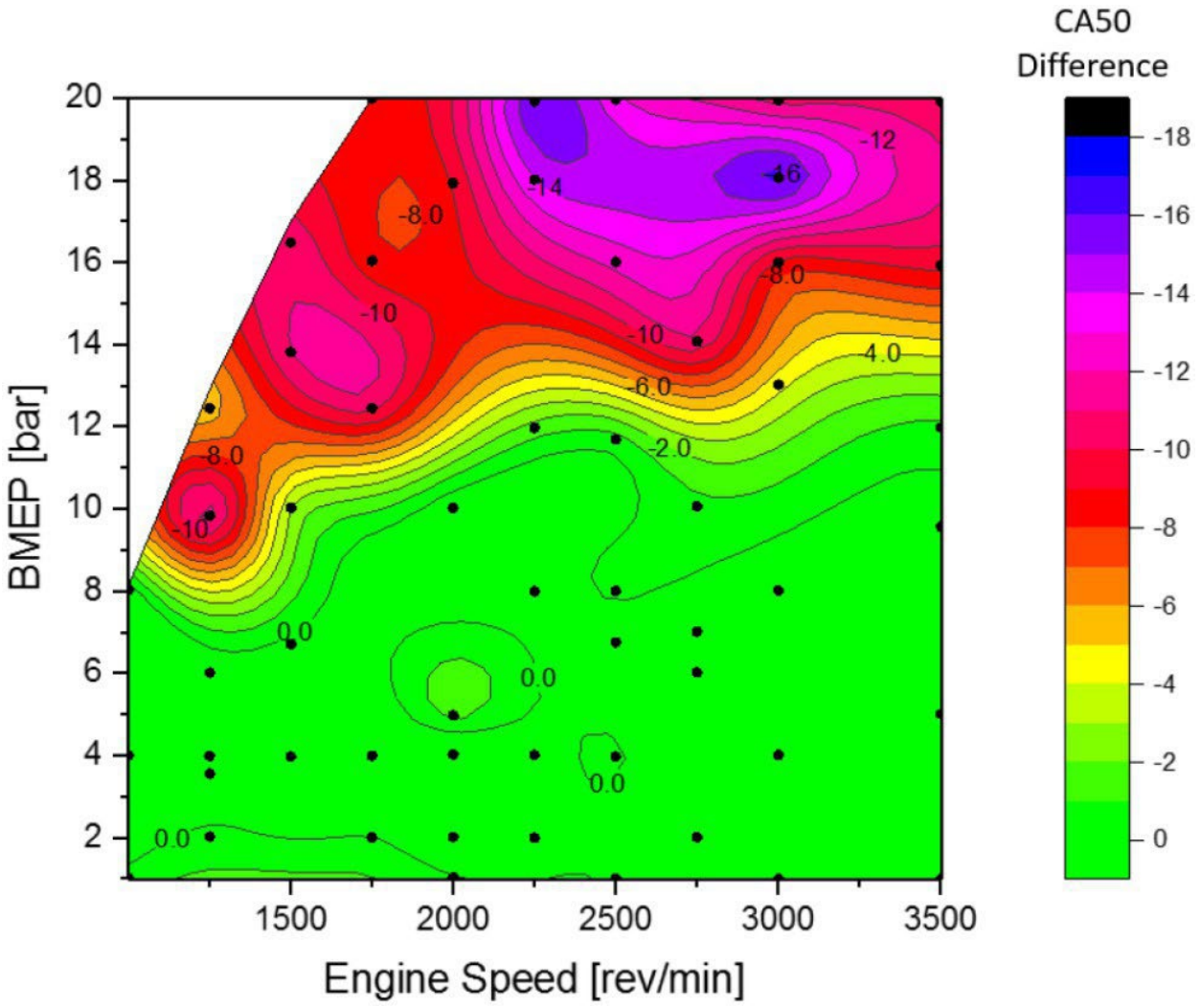

Figure 17 CA50 comparison map between 12.0:1 and 10.5:1 CR configurations, both with LP-EGR. Negative values denote that the CA50 for the 10.5:1 configuration was advanced compared to the high CR configuration

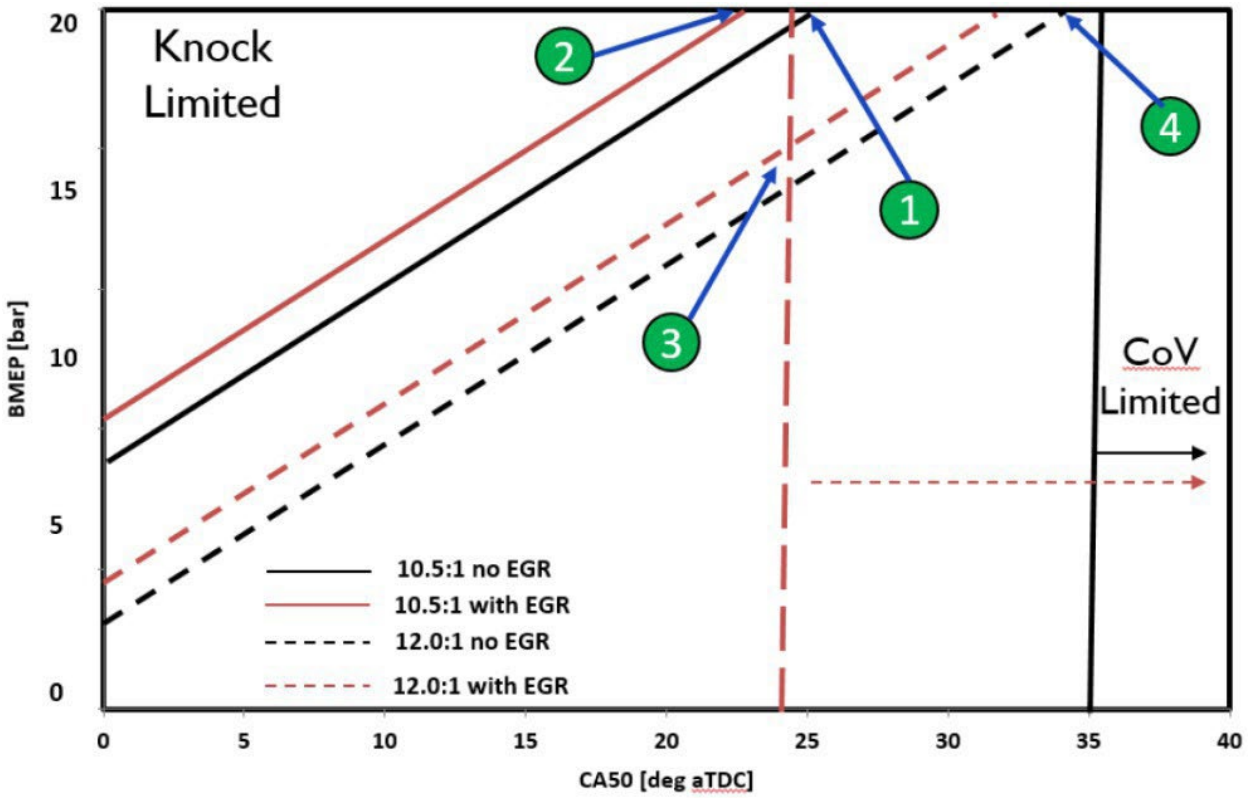

Figure 18 Representation of the Knock-Stability limited load point for high and low CR configurations with and without EGR.

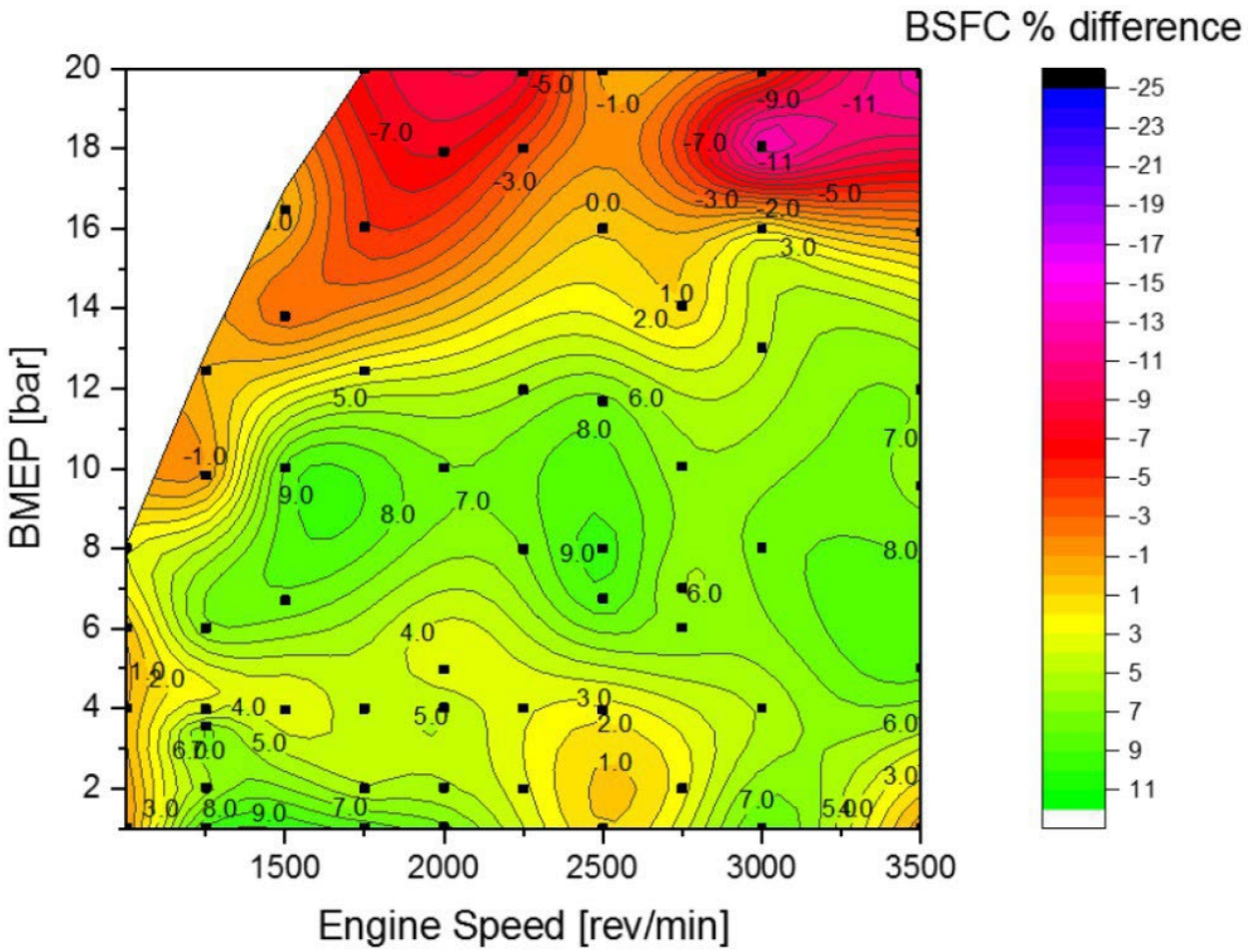

Figure 19 BSFC comparison map between CR 12.0:1 and CR 10.5:1 without EGR. Positive values indicate BSFC is lower for the CR 12.0:1 case.

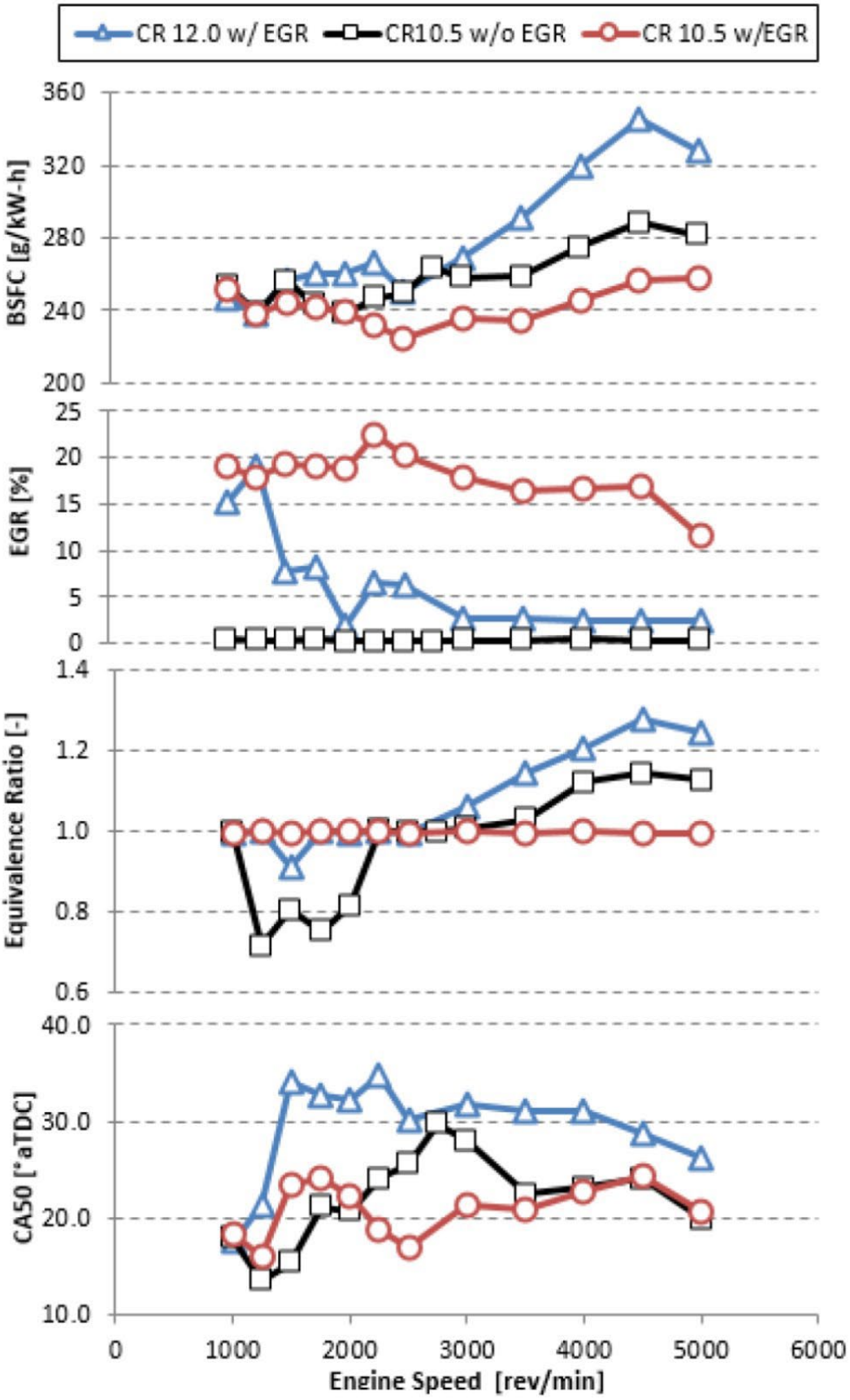

Figure 20 Full-load performance for the three test configurations

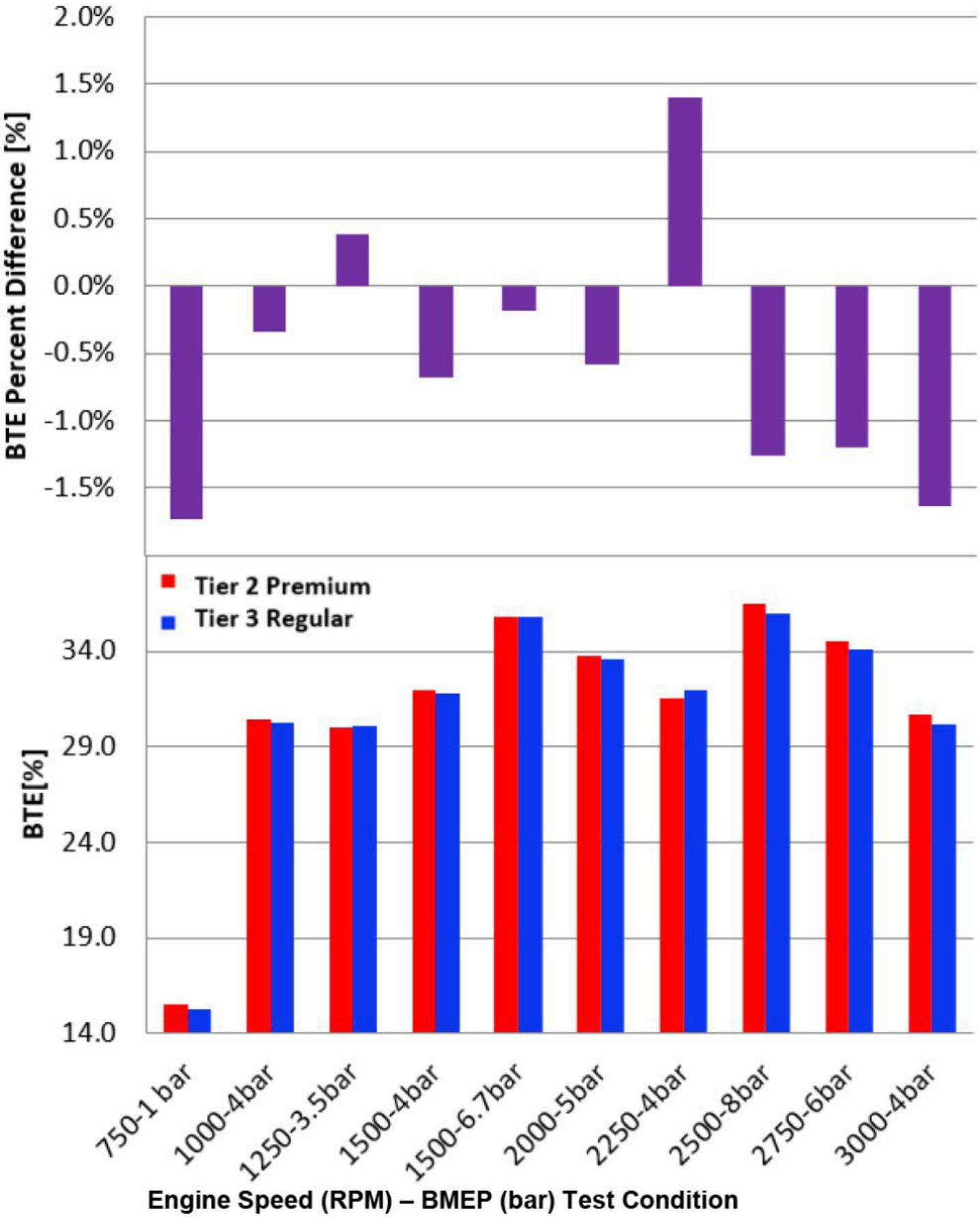

Figure 21 Part-load BTE comparison between Premium and Regular fuels. Negative BTE % difference values indicate higher BTE for the premium fuel.

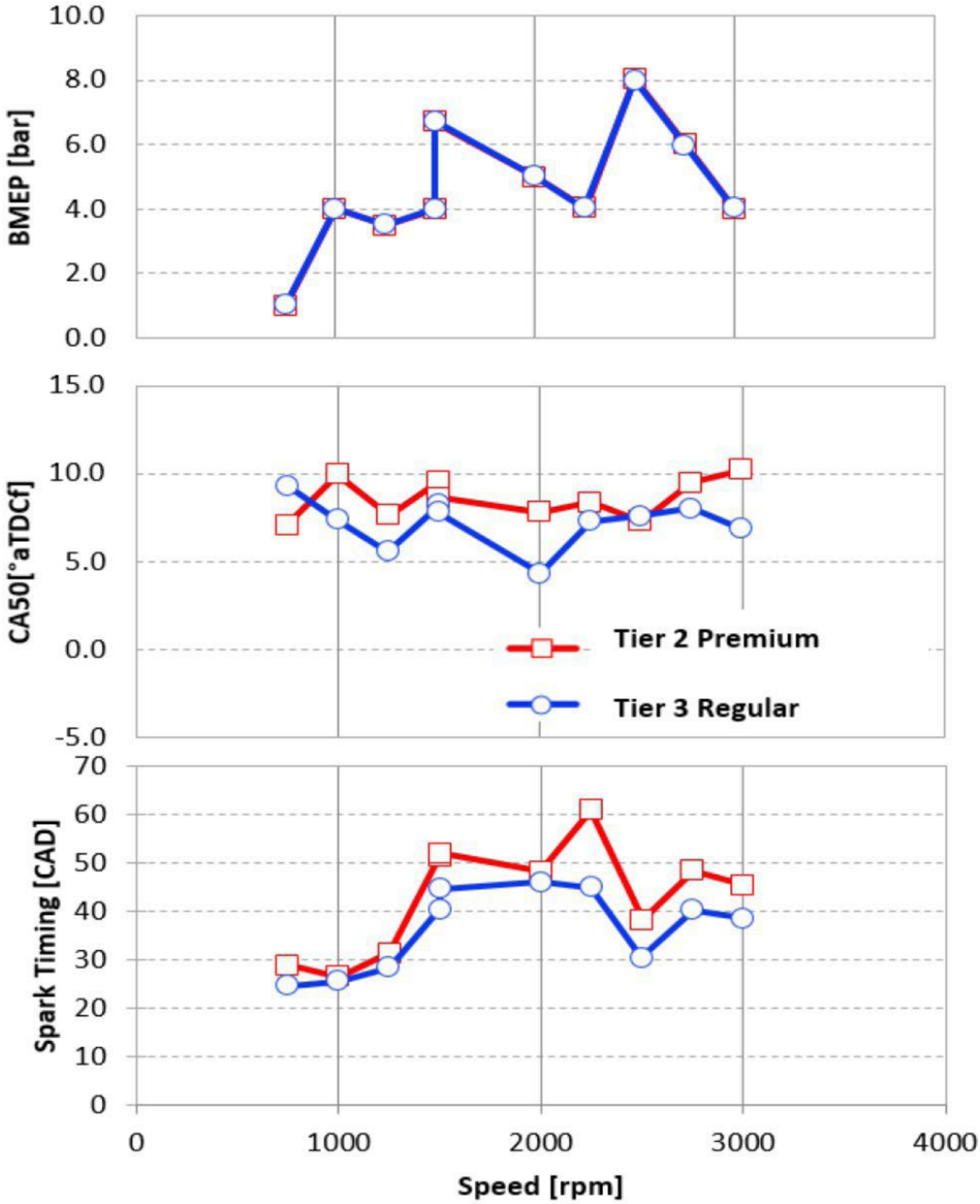

Figure 22 Comparison of spark timing and CA50 for two different fuels. The 0-50 CAD can be calculated by adding the sparking and CA50 values.

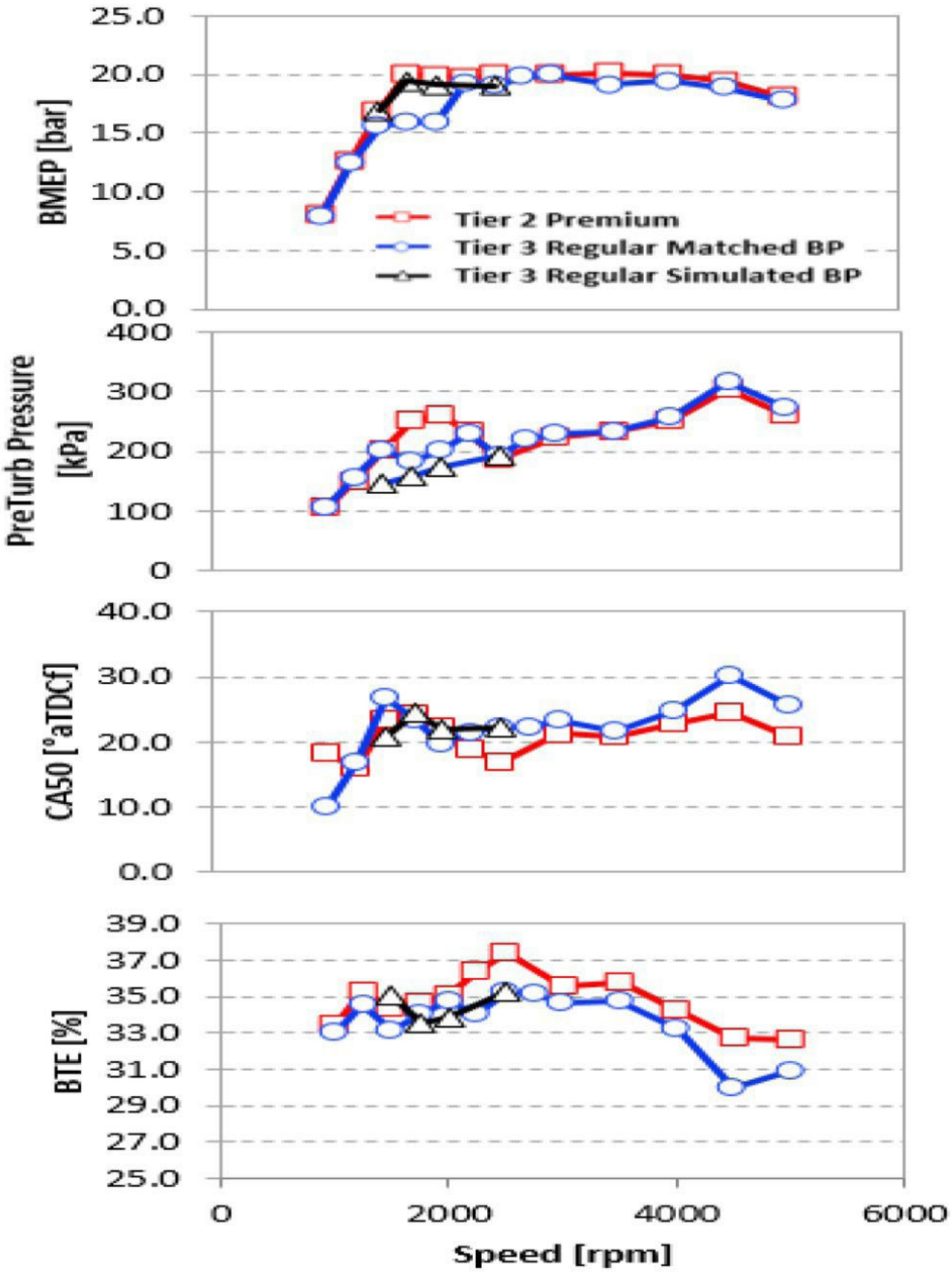

Figure 23 Full load performance data for the Tier 2 and LEV III fuels. Two back-pressure (BP) tests were run for the regular fuel. All points are data tested on engine hardware

Table 1. Engine Specifications

Displaced volume	1598 cc
Stroke	85.8 mm
Bore	77 mm
Compression ratio	10.5:1
Number of Valves	4
Fuel System	Side-Mounted GDI (120
Turbocharger	Single-Stage Twin Scroll
Rated Power	120 kW @ 5000 rpm
Rated Torque	275 Nm @ 1700 – 4500
Emissions Compliance	Euro V

Table 2. Fuel specifications

	EPA Tier II Certification Fuel	**LEV III Regular Certification**
Fuel Grade	Premium	Regular
Ethanol Content (vol %)	0	10
LHV (MJ/kg)	43.25	41.39
RON/MON/AKI	96 / 87.7 /	91.8 / 84.2 /
H:C	1.85	1.95
O:C	NA	0.0326
Total Aromatics (vol %)	28	22

Table 3 – EPA ALPHA vehicle model combined/weighted two-cycle GHG emissions results for the three PSA engine configurations using Tier 2 fuel.

Modeled Vehicle Specifications (MY2016 Mid-sized Light-Duty Passenger Car)								ALPHA Modeling Results	
Engine	Engine Scaling	Transmission	Trans. Torque Rating (N-m)	Test Weight (lbs.)	R.L. A Coeff. (lbf.)	R.L. B Coeff. (lbf/mph)	R.L. C Coeff. (lbf/mph^2)	Combined Cycle GHG (CO_2 g/mi)	% Change from Previous
2012 OEM PSA EP6CDTX	1.75L I4	6-sp. AT	321	3510	30.62	-0.0199	0.01954	238.6	--
SwRI EP6CDTX w/10.5:1 CR & LP-EGR	1.78L I4	6-sp. AT	328	3510	30.62	-0.0199	0.01954	231.0	-3.2%
SwRI EP6CDTX w/12:1 CR & LP-EGR	1.79L I4	6-sp. AT	329	3510	30.62	-0.0199	0.01954	225.2	-2.5%